

Audio-Visual Speaker Tracking: Progress, Challenges, and Future Directions

JINZHENG ZHAO¹, YONG XU², (Senior Member, IEEE),
XINYUAN QIAN³, (Senior Member, IEEE), DAVIDE BERGHI¹, (Student Member, IEEE),
PEIPEI WU¹, MENG CUI¹, JIANYUAN SUN⁴, PHILIP J.B. JACKSON¹, (Member, IEEE),
AND WENWU WANG¹, (Senior Member, IEEE)

¹Centre for Vision, Speech and Signal Processing, University of Surrey, Guildford, GU2 7XH, UK

²Tencent AI Lab, Bellevue, WA 98004, USA

³Department of Computer Science and Technology, University of Science and Technology Beijing, Beijing 100083, China

⁴Department of Computer Science, University of Sheffield, Sheffield, S1 4DP, UK

Corresponding author: Jinzheng Zhao (email: j.zhao@surrey.ac.uk).

This research is supported by Tencent AI Lab Rhino-Bird Gift Fund and University of Surrey.

ABSTRACT Audio-visual speaker tracking has drawn increasing attention over the past few years due to its academic values and wide application. Audio and visual modalities can provide complementary information for localization and tracking. With audio and visual information, the Bayesian-based filter can solve the problem of data association, audio-visual fusion and track management. In this paper, we conduct a comprehensive overview of audio-visual speaker tracking. To our knowledge, this is the first extensive survey over the past five years. We introduce the family of Bayesian filters and summarize the methods for obtaining audio-visual measurements. In addition, the existing trackers and their performance on AV16.3 dataset are summarized. In the past few years, deep learning techniques have thrived, which also boosts the development of audio-visual speaker tracking. The influence of deep learning techniques in terms of measurement extraction and state estimation is also discussed. At last, we discuss the connections between audio-visual speaker tracking and other areas such as speech separation and distributed speaker tracking.

INDEX TERMS Audio-Visual Speaker Tracking, Bayesian Filter, Sound Source Localization, Data Association, Face Detection

I. INTRODUCTION

The goal of speaker tracking is to determine the positions of the speaker in each time step using data from sensors like microphones and cameras. It has wide applications, including but not limited to human-computer interaction [1], speech recognition [2], speaker diarization [3], speech enhancement [4] and monitoring [5]. Besides, it has been employed to automatically extract tracking metadata for object-based media production [6], [7], where audio-visual objects are faithfully spatialized according to their position in space [8], [9].

The localization resolution of audio is low but audio can localize the speaker omnidirectionally. The localization resolution of visual signals is high but it can only localize the

speaker when the speaker is in the field of view. Thus audio provides a complementary modality to overcome limitations of visual modality under conditions like occlusion, field-of-view constraints, and poor illumination where visual cues degrade. On the contrary, when audio is affected by strong room reverberation and ambient noise, video information can serve as a backup. This indicates the collaborative potential of multiple modalities for improving tracking performance.

Audio-visual multi-speaker tracking presents several challenges requiring careful consideration, including (1) integrating the audio and visual data in a complementary manner, (2) estimating the number of simultaneous speakers which is unknown and dynamically changing [10], (3) dealing with many complex sources of uncertainty, such as missing

detections, noise, clutters, and absent modality, and (4) improving the tracking efficiency while maintaining the tracking accuracy.

There have been several surveys [11] before for audio-visual speaker tracking. Based on previous works, we give a more comprehensive and up-to-date literature review of the visual measurements generation, audio measurements generation, Bayesian trackers, datasets and metrics, including the works appearing recently. Techniques in [11] are mostly statistic-based, while we include more learning-based techniques in our survey such as learning-based audio-visual features and learning-based Bayesian filter.

The rest of the survey is listed as follows. In Section II, we recall the related techniques. Section III classifies the trackers into Bayesian trackers, learning-based trackers and differentiable Bayesian trackers, which are the hybrid of statistic-based tracking and learning-based tracking. Then we compare the performance of the current methods on AV16.3 dataset. In Section IV, we summarize the audio and visual features. In Section V and VI, we summarize the commonly used dataset and metrics. At last, we propose some future directions and conclude the survey.

II. Background

A. Difference between Localization and Tracking

Localization and Tracking are two related but distinct concepts. Localization refers to the process of determining the precise position of an object within a defined coordinate system. Localization is usually a one-time event, where the goal is to determine the current position accurately at a specific moment. While tracking involves continuously monitoring the movement and changes in the position of an object over time. Data association is often used to correspond the objects in the past time steps with the objects in the current time steps. Bayesian filter is often employed to model the state updating process.

In the task of audio-visual speaker tracking, measurement extraction and Bayesian estimation are two important steps as the quality of the measurements and state estimation based on the measurements determines the tracking accuracy.

B. Audio and Visual Measurements

For visual measurements, bounding boxes output by face detectors are widely used [12] [13] as face detectors can provide accurate detection results. The Color histogram [14] is another effective tool to provide visual measurements. It can also serve as complementary information for face detectors if the face detectors fail when the speakers' faces are not facing towards the camera or the illumination conditions are poor. Other traditional visual features such as the local binary patterns (LBPs) [15] and scale-invariant feature transform (SIFT) [16] can also be used.

For audio measurements, global coherence field (GCF) [17] can provide 2D or 3D coordinates as a direct position measurement. Sam-sparse-mean (SSM) [18] or MULTIPLE

Signal Classification (MUSIC) [19] can be used to provide estimates for the Direction of Arrival (DOA) of the speakers. In addition to the traditional sound source localization methods, learning-based methods have emerged in recent years, which aim to learn mappings from audio features to DOA or Cartesian coordinates [20].

C. Bayesian Filter

The objective of tracking is to obtain the joint probability of target states recursively. Kalman filter (KF) [21] is a popular solution to the task of tracking due to its high computational efficiency. KF assumes the motion of objects is linear and the posterior density is Gaussian. However, it does not always provide an optimal solution, due to its highly restrictive assumptions. In contrast, particle filters (PF) [22] are sequential Monte Carlo methods, which approximate the state distribution by a set of weighted particles through sequential importance sampling. Both the KF and PF algorithms require the number of targets to be fixed and known a priori. Thus they cannot deal with the scenarios of various and unknown numbers of speakers.

Random Finite Set (RFS) [23] is proposed to model the evolution of a time-varying number of objects by involving the process of motion, birth and death of targets, which lays foundations for the development of Probability Hypothesis Density (PHD) filter [24]. PHD filter propagates the first-order moment of the multi-target posterior. It has the form of linear Gaussian models, which can be regarded as the extension of Kalman filter from scenes of a single target to those of multiple targets, and the SMC form known as the SMC PHD filter, which approximates the posterior density by a set of particles. PHD filter estimates the number of targets by the mean of cardinality distribution. However, this estimation has a high variance if the number of targets is very large. To solve this problem, cardinalized PHD (CPHD) is proposed to propagate the intensity and cardinality distribution at the same time.

Different from PHD and CPHD filter, Multi-target multi-Bernoulli (MeMBeR) filter propagates the full posterior density, instead of the intensity [25]. The posterior density is represented as the Bernoulli RFS, which is null (meaning that the target disappears) or has a single element (meaning that the target exists). The predicted density includes the density of survived targets and newborn targets, while the updated density includes the density of legacy tracks and observation-corrected tracks. The number of tracks is estimated by the cardinality mean. Then, the corresponding number of tracks is selected by the order of existence probabilities. This process is advantageous to the PHD filter, where the tracks are clustered according to the estimated number of targets. This prediction can be inaccurate when the estimated number of targets is not equal to the natural number of clusters of particles. In addition, the clustering process is computationally inefficient. In [26], the existence of cardinality bias in MeMBeR was found and the cardinality balanced

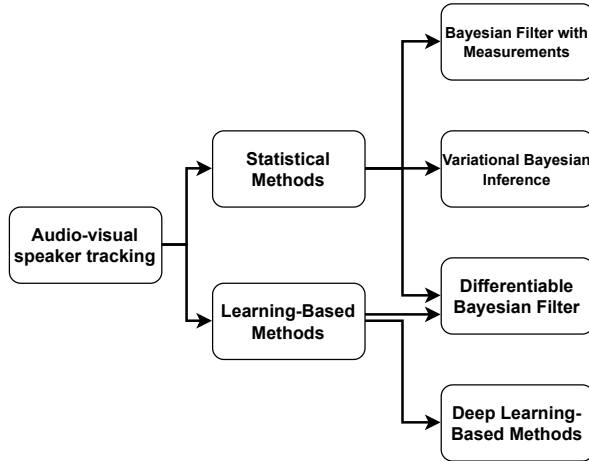


FIGURE 1. The Classification of Audio-Visual Trackers.

version (CBMeMber) was then proposed. The Bernoulli filters discussed above do not include label information. To solve this problem, Generalized Labeled Multi-Bernoulli filter (GLMB) [27] is proposed and incorporates the label information in the density.

The Poisson multi-Bernoulli mixture (PMBM) filter, proposed in [28] [29], leverages the conjugacy property that the predicted and updated distributions follow the same distribution. The conjugacy property enables efficient implementation. It represents undetected objects with a Poisson process and detected objects with a multi-Bernoulli mixture. Compared to other Bernoulli-based filters, PMBM has demonstrated superior performance in accuracy and speed [30]. In [31], PMBM is used for 3D tracking with measurements from a mono camera. In [32], PMBM is employed for vehicle tracking using LiDAR data.

III. Methods of Audio-Visual Speaker Tracking

The classification of the current audio-visual speaker tracker is shown in Fig. 1. As most trackers adopt the traditional statistical methods, or use the Bayesian filter with measurements, we start the survey with the Bayesian filter, and then we talk about some emerging techniques such as differentiable Bayesian filters and Transformer-based methods.

A. Bayesian Tracking

Bayesian based trackers aim to predict target states \mathbf{x}_k at time step k recursively given the measurements $\mathbf{z}_{1:k}$. It is assumed that the estimate of target states follows a Markov process of order one, i.e. \mathbf{x}_k only depends on \mathbf{z}_k and has no relevance with $\mathbf{z}_{1:(k-1)}$, as shown in Figure 2. Target states are defined as $\mathbf{x} = (x, v_x, y, v_y)$ in 2D tracking and $\mathbf{x} = (x, v_x, y, v_y, z, v_z)$ in 3D tracking (subscripts k omitted for convenience), where (x, y, z) is the position of the speaker's mouth and (v_x, v_y, v_z) is the velocity component. The estimation process contains two steps: prediction and update, as shown in Figure 3.

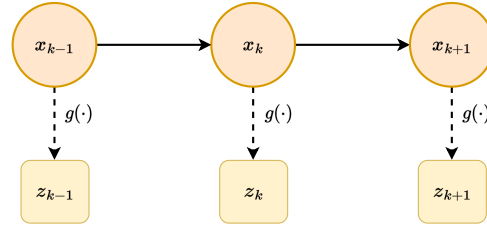


FIGURE 2. Illustrations of Hidden Markov Model

The predicted distribution $p_{k+1|k}(\mathbf{x}_{k+1})$ at time step $k+1$ can be derived by the Chapman Kolmogorov equation:

$$p_{k+1|k}(\mathbf{x}_{k+1}) = \int \pi(\mathbf{x}_{k+1} | \mathbf{x}_k) p_{k|k}(\mathbf{x}_k) \delta \mathbf{x}_k \quad (1)$$

where $\pi(\mathbf{x}_{k+1} | \mathbf{x}_k)$ is the transition density, assumed to have a constant velocity.

The updated distribution at time $k+1$ incorporating measurements \mathbf{z}_{k+1} can be calculated with the measurement model $g(\mathbf{z}_{k+1} | \mathbf{x}_{k+1})$:

$$p_{k+1|k+1}(\mathbf{x}_{k+1}) = \frac{g(\mathbf{z}_{k+1} | \mathbf{x}_{k+1}) p_{k+1|k}(\mathbf{x}_{k+1})}{\int g(\mathbf{z}_{k+1} | \mathbf{x}'_{k+1}) p_{k+1|k}(\mathbf{x}'_{k+1}) \delta \mathbf{x}'_{k+1}} \quad (2)$$

We summarize the Bayesian filters in Table 1.

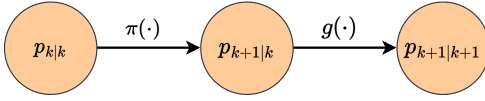
1) Kalman Filter

In Kalman filter [21], the posterior distribution $p_{k|k}(\mathbf{x}_k)$ and $p_{k+1|k+1}(\mathbf{x}_{k+1})$ are Gaussian and the transition process $\pi(\mathbf{x}_{k+1} | \mathbf{x}_k)$ is linear. Kalman filter gives optimal performance with linear Gaussian measurements and has been applied in audio-visual speaker tracking. In [33] and [34], a neural network was designed to determine the weights of audio and visual signals dynamically and Kalman filter is used to predict DOA adaptively. In addition to audio-visual speaker tracking, Kalman filter has been used in Multiple Object Tracking (MOT). In [35], SORT was proposed which combined Kalman filter with Hungarian algorithm [36] for motion prediction and data association. In [37], the same estimation model in [35] was employed and the appearance information of objects was integrated to improve the performance. In [37] and [35], the object motion is considered linear due to the high frame per second (FPS) of the camera.

Kalman filter is not applicable to non-linear measurements due to its use of linear and Gaussian models. Extensions of Kalman filter such as extended Kalman filter (EKF) [38] and unscented Kalman filter (UKF) [39] can handle non-linear measurements. EKF uses a local linearization by utilizing the first term in a Taylor expansion of the nonlinear function to deal with the non-linearity. UKF mitigates the problem of non-linearity by approximating the state distribution by a set of points. In [40], EKF was employed to process audio and visual measurements separately, and to fuse the two estimations at the decision level to obtain the final results.

TABLE 1. Overview of Bayesian Filters

Method	Propagating Representation	Prediction / Update Function	No. Targets
Kalman Filter	Gaussian Posterior	Linear	Single
Extended Kalman Filter	Gaussian Posterior	Nonlinear	Single
Unscented Kalman Filter	Gaussian Posterior	Nonlinear	Single
Particle Filter	SMC Posterior	Nonlinear	Multiple
GM-PHD	Gaussian Intensity	Linear	Multiple
SMC-PHD	SMC Intensity	Nonlinear	Multiple
GM-Bernoulli Filter	Gaussian Spatial PDF	Linear	Single
SMC-Bernoulli Filter	SMC Spatial PDF	Nonlinear	Single
PMBM Filter	Gaussian Multiple Bernoulli Mixture	Linear	Multiple


FIGURE 3. States Updating of Bayesian Filter

2) Particle Filter

Particle filter is a sequential Monte Carlo (SMC) algorithm and has better performance than EKF and UKF. However, PF suffers from a weight degeneracy problem if only a few particles contribute to the state estimation after several iterations. A resampling algorithm is proposed to mitigate the effect of degeneracy [22]. The main idea of resampling is to duplicate important particles and discard unimportant ones. The resampling methods include multinomial resampling, residual resampling [41], stratified resampling and systematic resampling [42]. However, resampling may create many repeated particles, which lowers their diversity. The traditional intelligent optimization algorithms can be combined with particle filters to maintain the diversity of particles such as particle swarm optimization algorithm [43] and firefly algorithm [44], [45].

In the general framework of a particle filter, there are four fundamental steps: initialization, prediction, update, and resampling. Particles, denoted as $\mathbf{p}_k^{(i)}$ at time step k , are employed to represent the state of an object, with i serving as the particle index. In the initial stage, all particles share the same weight, which is uniformly distributed as $w_0^{(i)} = \frac{1}{N}$ with N denoting the number of particles. In the prediction step, particle states are advanced by:

$$\mathbf{p}_k^{(i)} = \mathbf{F}\mathbf{p}_{k-1}^{(i)} + \mathbf{q}_k^{(i)} \quad (3)$$

where \mathbf{F} represents the prediction matrix and $\mathbf{q}_k^{(i)}$ denotes the Gaussian noise $\mathcal{N}(0, \mathbf{Q}^2)$.

In the update step, particles' weights are adjusted by the measurement model with measurements \mathbf{z}_k .

$$\omega_k^{(i)} \propto g(\mathbf{z}_k | \mathbf{p}_k^{(i)}) \quad (4)$$

Subsequently, speakers' states can be updated by the weighted average over the particle states:

$$\mathbf{x}_k = \sum_{i=1}^N \omega_k^{(i)} \mathbf{p}_k^{(i)} \quad (5)$$

The final step in the process is resampling, where particles with large weights are preserved and copied for the subsequent time step, while particles with small weights are removed. This step ensures that the particle set remains representative of the evolving state distribution.

3) RFS

Both the KF and PF algorithms assume that the number of tracking targets is known and fixed. If the number of targets varies with time, these algorithms may not work well. Random Finite Set (RFS) is proposed to model the evolution of objects with unfixed quantities. RFS depicts the process of motion, birth and death of targets.

From the perspective of RFS, for a target with the state \mathbf{x}_k at time k , it has the surviving possibility P_S to exist at time $k+1$ and evolves to the state \mathbf{x}_{k+1} with the transition function $\pi(\mathbf{x}_{k+1} | \mathbf{x}_k)$, or has the possibility $1 - P_S$ to die. At the same time, new targets may appear. The new targets come from two parts, namely, the targets spawned from the existing targets, and the born targets that are independent from the existing targets. Therefore, The multi-target states at time $k+1$ are from three aspects: surviving targets at time $k+1$, the spawned targets from time k and new born targets at time $k+1$.

The state distribution of measurements Z_k at time k also follows RFS. The target \mathbf{x}_k has the possibility P_D to be detected or has the possibility $1 - P_D$ to be missed. Apart from the measurements from the targets, the audio or visual sensors may generate clutter such as false positive detection.

4) PHD Filter

PHD filter is short for Probability Hypothesis Density Filter, which transmits the first-order moment of the posterior density to lower the computational complexity. The first-

order moment is also called the intensity v , whose integral is the estimated number of speakers. The PHD filter contains the prediction and update steps. The prediction is expressed as follows:

$$v_{k+1|k}(\mathbf{x}_{k+1}) = \gamma_{k+1}(\mathbf{x}_{k+1}) + \int p_S \pi_{k+1|k}(\mathbf{x}_{k+1} | \mathbf{x}_k) v_{k|k}(\mathbf{x}_k) d\mathbf{x}_k + \int \beta_{k+1|k}(\mathbf{x}_{k+1} | \mathbf{x}_k) v_{k|k}(\mathbf{x}_k) d\mathbf{x}_k \quad (6)$$

where $v_{k+1|k}(\mathbf{x}_{k+1})$ is the new speakers birth intensity and $\pi_{k+1|k}(\mathbf{x}_{k+1} | \mathbf{x}_k)$ is the states transition function defined as before. $\beta_{k|k-1}(\mathbf{x}_k | \mathbf{x}_{k-1})$ is the intensity of the speakers spawned from \mathbf{x}_k . The update process is expressed as follows:

$$v_{k+1|k+1}(\mathbf{x}_{k+1}) = (1 - p_D) v_{k+1|k}(\mathbf{x}_{k+1}) + \sum_{z_{k+1} \in \mathcal{Z}_{k+1}} \frac{p_D g_{k+1}(z_{k+1} | \mathbf{x}_{k+1}) v_{k+1|k}(\mathbf{x}_{k+1})}{\kappa_{k+1} + \int p_D g_{k+1}(z_{k+1} | \mathbf{x}_{k+1}) v_{k+1|k}(\mathbf{x}_{k+1})} \quad (7)$$

where p_D is the detection probability, $g_{k+1}(z_{k+1} | \mathbf{x}_{k+1})$ is the measurement likelihood function given measurements z_{k+1} , and κ_{k+1} is the clutter intensity.

The PHD filter has no closed-form solutions and only has two numerical solutions: the Gaussian mixture form (GM-PHD) [46] and the SMC form (SMC-PHD) [47]. The latter form has been widely used as it does not require the linear Gaussian assumption. Audio-visual SMC-PHD [48] filter is proposed for multiple speakers tracking using both audio and visual information. Audio information is used to relocate particles combined with particle flow [49] and to detect new speakers while the visual information is used to update the particle weights.

5) Bernoulli Filter

Bernoulli Filter is related to the Poisson RFS, the Bernoulli RFS and the multi-Bernoulli RFS.

a: Poisson RFS

The probability density function (pdf) $f(\mathbf{X})$ of a Poisson RFS X is as follows:

$$f(\mathbf{X}) = e^{-\lambda} \prod_{\mathbf{x} \in \mathbf{X}} \lambda p(\mathbf{x}) \quad (8)$$

where λ is the Poisson rate and $p(\mathbf{x})$ is the object pdf. The cardinality of a Poisson RFS follows Poisson distribution. The Poisson RFS is often used to describe clutter distribution.

b: Bernoulli RFS

The Bernoulli RFS has the possibility q to be empty and has the possibility $1 - q$ to have one element. The pdf $f(\mathbf{X})$ of a Bernoulli RFS \mathbf{X} is as follows:

$$f(\mathbf{X}) = \begin{cases} 1 - q, & \text{if } \mathbf{X} = \emptyset \\ q \cdot p(\mathbf{x}), & \text{if } \mathbf{X} = \{\mathbf{x}\} \end{cases} \quad (9)$$

where $p(\mathbf{x})$ is the object pdf and $0 \leq q \leq 1$.

c: Multi-Bernoulli RFS

The multi-Bernoulli RFS \mathbf{X} is composed of N independent Bernoulli RFSs \mathbf{X}_i :

$$\mathbf{X} = \bigcup_{i=1}^N \mathbf{X}_i \quad (10)$$

where \mathbf{X} can be determined by $\{(q^{(i)}, p^{(i)})\}_{i=1}^N$, where q and p are defined in Section b. The pdf of a multi-Bernoulli RFS is defined as follows:

$$f(\mathbf{X}) = \prod_{j=1}^N (1 - q^{(j)}) \times \sum_{1 \leq i_1 \neq \dots \neq i_m \leq N} \prod_{j=1}^m \frac{q^{(i_j)} p^{(i_j)}(x_j)}{1 - q^{(i_j)}} \quad (11)$$

Equation (11) traverses all circumstances that m RFSs have one element and the remaining $N - m$ RFSs are empty.

d: Multi-target Multi-Bernoulli (MeMBer) Filter

Suppose the pdf of a multi-Bernoulli RFS at time k can be represented as follows:

$$f_k = \left\{ \left(q_k^{(i)}, p_k^{(i)} \right) \right\}_{i=1}^{N_k} \quad (12)$$

The predicted pdf is the union of the surviving Bernoulli targets and the new born Bernoulli targets:

$$f_{k+1|k} = \left\{ \left(q_{P,k+1|k}^{(i)}, p_{P,k+1|k}^{(i)} \right) \right\}_{i=1}^{N_k} \cup \left\{ \left(q_{\Gamma,k+1}^{(i)}, p_{\Gamma,k+1}^{(i)} \right) \right\}_{i=1}^{N_{\Gamma,k+1}} \quad (13)$$

where $(q_{P,k+1|k}^{(i)}, p_{P,k+1|k}^{(i)})$ are the parameters of the surviving targets and $N_{\Gamma,k+1}$ is the number of new born targets with parameters $(q_{\Gamma,k+1}^{(i)}, p_{\Gamma,k+1}^{(i)})$. The predicted pdf in Equation (13) can be simplified as follows:

$$f_{k+1|k} = \left\{ \left(q_{k+1|k}^{(i)}, p_{k+1|k}^{(i)} \right) \right\}_{i=1}^{N_{k+1|k}} \quad (14)$$

The updated pdf at time $k + 1$ can be approximated by the union of the legacy tracks and the measurement-corrected tracks:

$$f_{k+1} \approx \left\{ \left(q_{L,k+1}^{(i)}, p_{L,k+1}^{(i)} \right) \right\}_{i=1}^{N_{k+1|k}} \cup \{(q_{U,k+1}(z), p_{U,k+1}(\cdot; z))\} z \in Z_{k+1} \quad (15)$$

where $(q_{L,k+1}^{(i)}, p_{L,k+1}^{(i)})$ is the parameters of the legacy tracks and $(q_{U,k+1}(z), p_{U,k+1}(\cdot; z))$ is the parameters of the measurement-corrected tracks with Z_{k+1} being the measurement set. The detailed calculation of Equation (13) and Equation (15) can be found in [26].

6) PMBM Filter

PMBM filter was proposed in [28] [29]. In each time step, PMBM filter manages the distribution of targets in two categories. The first part is targets that have been successfully associated with measurements obtained from sensors. The

others are targets that exist but have not been associated with any measurements. The distribution of detected targets is represented by a multiple Bernoulli mixture distribution, denoted as $f(\cdot)$, which encapsulates all the information regarding the state and properties of detected targets. The distribution of undetected targets is modeled as a Poisson point process, represented by $\mu(\cdot)$. This distribution characterizes the spatial and temporal randomness associated with undetected targets. The set of all existing targets, denoted as \mathbf{x} , can be partitioned into two disjoint subsets: the detected targets (\mathbf{x}^d) and the undetected targets (\mathbf{x}^u). This partition is expressed as $\mathbf{x}^u \uplus \mathbf{x}^d = \mathbf{x}$. The PMBM density is calculated as the convolution of $\mu(\cdot)$ and $f(\cdot)$:

$$p_k(\mathbf{x}) = \sum_{\mathbf{x}^u \uplus \mathbf{x}^d = \mathbf{x}} \mu_k(\mathbf{x}^u) f_k(\mathbf{x}^d) \quad (16)$$

The predicted density for undetected targets and detected targets is handled independently.

- For undetected targets, the prediction density combines the birth intensity of new targets with the predicted density of existing targets that were undetected, which is scaled by surviving probability P^S .
- For detected targets, Kalman filter is employed, which takes into account the dynamics and uncertainties associated with each detected target.

The update step of the PMBM filter deals with the incorporation of new measurements and the adjustment of target states. The states of targets can be categorized into four types.

- For undetected targets that are misdetected again, the density is decreased by a factor of $(1 - P^D)$ to account for the probability of misdetection.
- For undetected targets detected for the first time or clutter, new Bernoulli distributions are introduced to represent these states. These Bernoulli distributions encapsulate the uncertainty associated with whether a new target is a true target or a clutter.
- For detected targets which are detected again, the density can be updated by Kalman filter with measurements.
- For detected targets which are misdetected, their states remain unchanged.

In PMBM, different data associations are different global hypotheses, represented by a multi-Bernoulli RFS mixture. Within the mixture, a multi-Bernoulli RFS represents one possible data association. Within the multi-Bernoulli RFS, one Bernoulli RFS represents a potential speaker. The global hypothesis with low weights will be pruned and similar global hypotheses will be merged for reducing the computational cost.

7) Variational Bayesian Inference

In [50], the problem of audio-visual speaker tracking is formulated as a temporal graphical model with latent variables. The objective is to maximize the posterior joint distribution of the latent variables based on the audio and visual measurements. Variational expectation maximization is used to deal with the intractable estimation. First, the expectation with regard to the latent variables is calculated for the posterior likelihood. Then the posterior likelihood is maximized to estimate the model parameters.

B. Tracking with Deep Learning

Most of the existing works for audio-visual speaker tracking employ Bayesian filters for data association and track management but very few works tried to use deep learning. The main reason is that the audio-visual speaker tracking datasets listed in Section V are not large enough to train a tracking network.

Several works on similar tasks have tried to use deep learning frameworks for tracking. In [51], an end-to-end framework is proposed for tracking on KITTI Tracking Benchmark [52], in which images of the visual and LiDAR modalities are provided. The proposed tracking framework ensembles feature extraction, data association and track management. In addition, in the MOT challenge, there are some works [53] [54] using RNN for a unified end-to-end tracking framework. Trackformer is proposed in [55], which is based on Transformer. The encoder takes the image as input and the decoder takes object queries as input. Each query corresponds to a potential object. The output of the decoder which indicates the appearance of the object will be delivered to the next time step as new queries. TransTrack [56] leverages two sets of queries. The one is object query, acting as an object detector. The other is track query, which associates objects in the current frame with those in previous frames. IOU matching is employed to associate the detected objects with tracklets. ByteTrack is proposed in [57]. Different from previous trackers, ByteTrack not only associates high confidence bounding boxes but the low confidence boxes. In MotionTrack [58], an interaction module is designed for short-term association and a re-find module is designed for long-term matching, which achieves a good performance under dense crowds and occlusions. In other survey papers [59], [60] with regard to MOT, more deep learning-based trackers are provided. In other tracking tasks such as 3D MOT [61] and infrared tracking [62], deep learning-based are also widely adopted.

More recently, AVRI [63] dataset has been proposed for audio-visual speaker localization and tracking. It contains more than nine hours of audio-visual data and enables the employment of deep learning techniques. However, AVRI can only be used for single-speaker tracking. Overall, using deep learning for audio-visual speaker tracking remains an open and challenging problem. The problem of the lack of large amounts of datasets needs to be overcome.

C. Differentiable Bayesian Filter

1) Learnable Prediction and Updating

Bayesian filters can also be designed to be differentiable so that the motion model in the prediction stage and the measurement-correct model in the update stage can be trained and optimized end-to-end through deep learning models. The transition model (Equation 1) and update model (Equation 2) can be replaced by deep learning modules.

$$p_{k+1|k}(\mathbf{x}_{k+1}) = T(p_{k|k}(\mathbf{x}_k)) \quad (17)$$

$$p_{k+1|k+1}(\mathbf{x}_{k+1}) = F(\mathbf{z}_{k+1}, p_{k+1|k}(\mathbf{x}_{k+1})) \quad (18)$$

where $T(\cdot)$ and $F(\cdot)$ denote the learnable transition and update model, which can be fed forward layers, convolutional neural networks, recurrent neural networks or Transformer modules. Compared to traditional Bayesian filters, the learnable models are more flexible to adapt to different scenarios.

2) Soft-Resampling

In particle filter, resampling is required to select the important particles and discard the low-weight particles. However, the resampling operation is not differentiable. To solve this problem, soft-resampling is proposed, which introduces a unified distribution $u(\cdot)$ mixed with updated particle distributions $p(\cdot)$.

$$q(i) = \alpha p(i) + (1 - \alpha)u(i) \quad (19)$$

where $0 < \alpha < 1$ is the hyperparameter. New particles are sampled from the new distributions $q(\cdot)$ instead of $p(\cdot)$. The weights of new particles are computed as follows:

$$\hat{w}_t^k = \frac{p(k)}{q(k)} = \frac{w_t^k}{\alpha w_t^k + (1 - \alpha)1/K} \quad (20)$$

With soft-resampling, particle filter can be designed to an end-to-end differentiable architecture.

3) Summarizations of Current Differentiable Bayesian Trackers

We summarize the differentiable Bayesian filters in Table 2. In [64], the differentiable Kalman filter is proposed. In [65], a review of deep learning methods combining the Kalman filter is presented. In [66], a differentiable particle filter was proposed and applied in visual odometry task [67]. The proposed differentiable model excludes the resampling part, which may ignore the effects of estimations in the last time step on the estimations in the current time step. In [68], a differentiable particle filter was applied in robot visual localization but with a differentiable soft-resampling step, which is beneficial for future estimations. These works show that the Bayesian algorithm priors (i.e., the prediction and the update) enable the explainability of the network, benefit the training process and lead to superior performance compared to pure deep learning models such as LSTM. In [69], a novel differentiable resampling technique is designed based on the weighted multi-head attention, which is superior to

the conventional resampling methods such as soft resampling and systematic resampling.

TABLE 2. Summarization of Differentiable Bayesian Filters. (FC denotes the fully connected layer, TRN denotes Transformer.)

Ref	Backbone	Bayesian Filter	Tasks
[64]	FC	Kalman Filter	State Estimation
[34]	FC	Kalman Filter	Speaker Tracking
[68]	CNN	Particle Filter	Visual Localization
[66]	CNN	Particle Filter	Global Localization
[70]	RNN	Particle Filter	Robot Localization, Sequence Prediction
[69]	TRN	Particle Filter	Resampling
[71]	RNN	Kalman Filter	Echo Cancellation
[72]	RNN	Kalman Filter	Noise Estimation
[73]	TRN	Particle Filter	Speaker Tracking

D. Summarization of Current Trackers

We summarize the audio-visual speaker trackers in the past few years in Table 3. We also summarize the MAE results of current trackers on AV16.3 dataset. The results on multiple speakers sequences are shown in Table 4. In [75], the number of speakers is known as a priori. This algorithm used color histograms as visual measurements and focused on the particles near the DOA lines. The SMC-PHD filter in [75] achieved the best performance in most sequences. As a following work, [76] solved the problem of audio-visual speaker tracking with an SMC-PHD filter, which does not need to know the number of speakers as a priori. Mean-shift algorithm [87] was further employed to move the particles closer to the speakers' locations. In [88], GCF is used to calculate sound source positions as audio measurements and utilized face detectors to derive the mouth positions as visual measurements. GLMB filter was employed to fuse the two modalities and generate the trajectories. In [74], dictionary learning is used to model the appearance of speakers and used PF as the tracking framework. DOA lines are used in this algorithm for the initialization of particle positions. The MAE results on single speaker sequence are shown in Table 5. In [77], an adaptive PF is designed where the covariance of the measurement likelihood function can change dynamically according to the reliability of the measurements. In [80], a two-layer PF is designed for 3D single-speaker tracking. The designed two-layer architecture increases the particle diversity. The particle weights are adjusted according to the confidence of audio and visual modalities. In [83], a multi-modal perception network is proposed to determine the weights of audio and visual measurements in a self-supervised way. In [82], a novel PF is proposed, which performs audio azimuth relocation and audio-visual azimuth-elevation relocation. Face detection is employed to estimate the distance. The measurement likelihood is derived based on the angle likelihood and the distance likelihood.

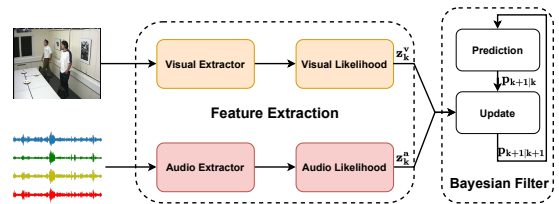
TABLE 3. Overview of methods (No. Spk denotes the maximum number of speakers. H denotes the color histogram, FD denotes the number of face detection, DLM denotes dictionary learning measurement and SR denotes Self-Recorded.)

Ref	Publication	Year	Backbone	Audio Feature	Visual Feature	Output	Dataset	No. Spk
[40]	IET	2012	EKF	GCC-PHAT	Mean Shift	2D	SR	2
[74]	TMM	2014	PF	DOA	DLM	3D	AV16.3 CLEAR EPFL	5
[75]	TMM	2015	PF	DOA	H	2D	AV16.3	3
[76]	TMM	2016	SMC-PHD	DOA	H	2D	AV16.3 AMI CLEAR	4
[77]	ICASSP	2017	PF	GCF	FD, H	3D	AV16.3	1
[78]	ICASSP	2018	PF	GCF	FD, H	3D	AV16.3 CAV3D	3
[12]	TMM	2019	PF	GCF	FD, H	2D, 3D	AV16.3 CAV3D	3
[79]	TMM	2019	SMC-PHD	DOA	FD, H	2D, 3D	AV16.3 AVDIAR CLEAR	4
[80]	ICIP	2019	PF	SSM	H	3D	AV16.3	3
[50]	TPAMI	2019	EM	DP-RTF	FD	2D	AV16.3 AVDIAR	4
[81]	INTER-SPEECH	2020	GLMB	GCF	FD	2D, 3D	AV16.3	3
[34]	ICASSP	2020	KF	SRP-PHAT	Facial Landmarks	DOA	SR	1
[82]	ICPR	2021	PF	GCF	FD, H	3D	AV16.3 CAV3D	3
[83]	AAAI	2022	PF	stGCF	Siamese Network	2D	AV16.3	1
[10]	ICASSP	2022	PMBM	DOA	FD	2D	AV16.3	3
[84]	INTER-SPEECH	2022	PMBM	GCF	FD	3D	AV16.3	3
[63]	TASLP	2023	Transformer	GCC-PHAT	FD	DOA	AVRI	1
[85]	SENSORS	2023	PF	GCC-PHAT	FD, H	2D, 3D	AV16.3 CAV3D	3
[86]	TMM	2023	SMC-PHD	DOA	FD	2D	AV16.3 AVDIAR CLEAR	4

We also summarize the performance of trackers on CAV3D dataset [12]. The metrics on the image plane and 3D space can be found in TABLE 6 and TABLE 7, respectively. We report the performance on single object tracking (SOT) sequences and multiple object tracking (MOT) sequences separately. SOT sequences refer to sequence 06 ~ 13 and sequence 20. MOT sequences refer to sequence 22 ~ 26. It is found that the MAE on CAV3D dataset is higher than that on AV16.3 dataset. As CAV3D is more challenging, it has stronger reverberation and more scenarios of occlusions and out-of-views.

IV. Measurements

Both audio and visual modalities can serve as measurements for tracking, as depicted in Figure 4. As pointed out by [88], the measurement likelihoods can be classified as generative

**FIGURE 4.** The structure of audio-visual speaker tracker.

or discriminative. The former calculates the possibility map in the feature space and finds the most possible regions where speakers will appear, which can be regarded as a similarity matching problem. The latter often employs a pretrained detector to locate speakers and give coordinates as direct measurements.

TABLE 4. Tracking results on multiple speaker sequences of AV16.3 datasets. The bold numbers indicate the best tracker for a given sequence and a given camera.

Sequence	Camera	Trackers			
		AV-A-PF [75]	AVMS SMC-PHD [76]	AV-GLMB [81]	Tracker [74]
Seq18-2p-0101	Cam1	14.31	-	15.7	-
	Cam2	11.66	-	10.9	-
	Cam3	15.80	-	6.3	-
Seq19-2p-0101	Cam1	11.88	-	15.3	-
	Cam2	9.62	-	11.6	-
	Cam3	12.08	-	5.4	-
Seq24-2p-0111	Cam1	9.95	13.93	16.5	22.28
	Cam2	8.85	14.97	10.6	17.60
	Cam3	10.02	14.12	7.0	28.18
Seq25-2p-0111	Cam1	14.78	15.72	17.7	21.49
	Cam2	7.70	13.93	10.8	19.17
	Cam3	8.93	17.07	10.7	29.35
Seq30-2p-1101	Cam1	13.84	16.65	14.8	35.98
	Cam2	8.85	14.86	10.4	28.40
	Cam3	10.30	19.29	15.7	34.60
Seq40-3p-0111	Cam1	12.38	-	-	-
	Cam2	12.04	-	-	-
	Cam3	11.30	-	-	-
Seq45-3p-1111	Cam1	16.35	22.95	-	-
	Cam2	17.22	21.47	-	-
	Cam3	13.84	22.43	-	-

TABLE 5. Tracking results on single speaker sequences of AV16.3 datasets. The bold numbers indicate the best tracker for a given sequence and a given camera.

Sequence	Camera	Trackers				
		AV-A-PF [75]	AV3D [77]	2LPF [80]	MPT [89]	Tracker [82]
Seq08-2p-0100	Cam1	10.75	4.31	3.32	3.67	3.01
	Cam2	7.33	4.66	3.08	3.58	2.30
	Cam3	9.85	5.34	3.47	3.43	3.59
Seq11-2p-0100	Cam1	14.66	8.15	6.15	6.77	5.43
	Cam2	14.01	7.48	5.58	4.55	4.60
	Cam3	13.96	6.64	3.86	3.84	6.28
Seq12-2p-0100	Cam1	12.49	6.86	4.11	4.67	4.23
	Cam2	10.81	10.67	5.39	4.84	4.53
	Cam3	11.86	9.71	5.65	3.78	4.25
Average		11.74	7.09	4.51	4.34	4.25

TABLE 6. 2D metrics on CAV3D datasets. The bold numbers indicate the best tracker.

Sequences	Metrics	Trackers		
		Tracker [82]	AV3T [12]	GAVT [85]
SOT	TLR	2.50	7.00	13.93
	MAE	12.00	16.50	26.76
MOT	TLR	-	11.20	21.01
	MAE	-	24.80	13.47

TABLE 7. 3D metrics on CAV3D datasets. The bold numbers indicate the best tracker.

Sequences	Metrics	Trackers		
		Tracker [82]	AV3T [12]	GAVT [85]
SOT	TLR	20.70	31.80	30.07
	MAE	0.21	0.30	0.29
MOT	TLR	-	35.70	32.01
	MAE	-	0.37	0.32

A. Visual Measurements

Visual modality is superior to audio modality in terms of localization accuracy as it can offer richer information. Face detectors and color histograms are often employed to extract features from images.

1) Face Detectors

As deep learning technologies thrive, face detectors are becoming quicker, stronger, and more robust. They provide coordinates of speakers' faces and discriminative likelihoods. MXNet [90] was used in [12] and [88] for detection and the dual shot face detector (DSFD) [91] was employed in [10] to provide mouth positions.

In addition to face detectors, object detectors like SSD [92] and person detectors like [93] can also be used in audio-visual tracking [50], [94]. After obtaining the coordinates of bounding boxes, some work [63], [95] encodes them to Gaussian vectors which represent the posterior distribution of the object positions along the horizontal and vertical axis.

2) Color Histogram

Color histogram methods can provide generative visual likelihoods by comparing the similarities between the reference image and the whole image search space. The reference images are often selected from the initial frame where speakers appear in a consecutive sequence. Color spatiogram [14] is an alternative [77], [78], which is enhanced by spatial means and covariance for each histogram bin to give a richer representation. Color histogram methods have been widely used [75], [76] to provide visual measurements. In scenarios where face detectors fail, color histogram methods can provide similarity feature maps as complementary information. The commonly used color representation is RGB and HSV. The similarity between two HSV histograms is calculated based on the Bhattacharyya distance:

$$D = \sqrt{1 - \sum_{n=1}^N \sqrt{r(n)q(n)}} \quad (21)$$

where N is the number of histogram bins, $r(n)$ is the Hue histogram of the reference image. The reference image is often selected as the initial frame where the speaker is visible. $q(n)$ is the Hue histogram of the search area.

3) Learning-Based Features

Another option is to provide a generative visual likelihood with a learning method, such as the Siamese Network [96]. Similar to color histograms, the similarity between the reference image and the search area is calculated on the learned features extracted with deep learning methods. For example, [89] adopts a pretrained fully-convolutional siamese network [97] to calculate the response map which is then used as the visual measurement.

B. Audio Measurements

Audio-visual speaker tracking relies on sound source localization (SSL) algorithms to obtain measurements by detecting and localizing the active sound sources. SSL methods can be broadly categorized into two groups: parametric-based methods and learning-based methods.

1) Parametric-Based Methods

Parametric-based methods typically rely on Time Difference of Arrival (TDOA) estimation [98], which often requires a computationally expensive global maximum search [99]. They work well under general conditions but tend to fail in the presence of strong reverberation and noise.

a: Global Coherence Field

Estimating the TDOA between different microphones provides useful spatial information for localization. Generalized Cross Correlation (GCC) is used for TDOA estimation but struggles when encountering background noise and room reverberation. To mitigate this problem, compared to GCC, Generalized Cross Correlation with Phase Transform (GCC-PHAT) is normalized by the magnitude while retaining the phase information, which is more robust under a bad environment [100]. Global coherence field (GCF) [17] gathers the spatial information by adding up GCC-PHAT of all microphone pairs. Peaks in the GCF map indicate the most likely position of the dominant speaker.

The computation of the Global Coherence Field (GCF) involves two steps. Firstly, GCC-PHAT is calculated for the j -th pair of audio recorded in the microphone array, denoted as $s_j \in S$, at time t . This calculation is defined as follows:

$$G_j(\tau, t) = \int_{-\infty}^{+\infty} \frac{\mathcal{F}_{s_{j,1}}(t, f) \mathcal{F}_{s_{j,2}}^*(t, f)}{|\mathcal{F}_{s_{j,1}}(t, f)| |\mathcal{F}_{s_{j,2}}^*(t, f)|} e^{j2\pi f\tau} df \quad (22)$$

where τ represents the inter-microphone time lag, f denotes the frequency, \mathcal{F} is short for the Short-Time Fourier Transform, $s_{j,1}$ and $s_{j,2}$ are the two microphones within the j -th pair, and $*$ signifies the complex conjugate. By summing the GCC-PHAT values across all pairs with the number of $|S|$, the final GCF is obtained.

$$GCF(\mathbf{p}, t) = \frac{1}{|S|} \sum_{n=1}^{|S|} G_n(\tau_n(\mathbf{p}), t) \quad (23)$$

where \mathbf{p} denotes discrete points sampled in the search space. The discrete point resulting in the maximum of GCF is regarded as the sound source.

b: Visual-Assisted Global Coherence Field

As indicated in [12], the accuracy of GCF estimations depends on the microphone array configuration. The distance between the speakers and the microphone array can not be estimated accurately with a small circular array. To mitigate this problem, the calculation of GCF can be assisted by the visual modality. The height of speakers z can be estimated by projecting the coordinates derived from face detection to 3D space. And the visual-assisted GCF is calculated by:

$$GCF(\mathbf{p}, t) = \frac{1}{|S|} \sum_{n=1}^{|S|} G_n(\tau_n(\mathbf{p}|z), t) \quad (24)$$

which reduces the search space from 3D space to 2D space and overcomes the limitations of the distance estimations.

c: GCC-PHAT de-emphasis

GCC-PHAT de-emphasis [101] is proposed for adapting GCC-PHAT to scenarios of multiple speakers. After localizing the dominant speaker using GCF, the time lag corresponding to the dominant speaker is masked and GCF is re-calculated using the masked GCC-PHAT for localizing the non-dominant speakers. However, as indicated in [88], GCC-PHAT de-emphasis does not perform well with the increasing number of speakers. And as shown in [84], even in the two-speaker scenario, the performance of GCC-PHAT de-emphasis is not satisfactory when the speakers are close to each other.

d: stGCF

There are additional GCF derivatives. For instance, [89] proposed space-temporal GCF (stGCF), which inserts spatial and temporal information assisted by visual modality and improves localization accuracy.

Assume $\mathbf{Q}^{2d} = \{q_{11}^{2d}, \dots, q_{wh}^{2d}\}$ is the sampling points across the image plane. Through the camera projection model [102], the 2D sampling points can be converted to groups of 3D points $\mathbf{Q}_k^{3d} = \{q_{11k}^{3d}, \dots, q_{whk}^{3d}\}$ with different depths $\mathbf{D} = \{d_1, \dots, d_k, \dots, d_L\}$.

$$\mathbf{Q}_k^{3d} = \Phi(\mathbf{Q}^{2d}, \mathbf{D}) \quad (25)$$

Then we obtain the GCF in different depth $GCF(\mathbf{Q}_k^{3d}, t)$. The spatial GCF is defined as $GCF(\mathbf{Q}_{k_m}^{3d}, t)$ where the maximum of GCF is achieved on the k_m -th depth. The spatial GCF is obtained over frames in $[t - n_1]$. Then the first n_2 largest spatial GCF is selected as spatial-temporal GCF.

Apart from GCF, other algorithms such as MUSIC [19], independent component analysis [103], and logistic regression [104] can also be used for providing audio measurements.

2) Learning-Based Methods

Learning-based methods are emerging as deep learning techniques thrive, which predict DOA [105] or Cartesian coordinates [106] [107] through neural networks trained to learn the mapping function that relates audio input features to the sound source positions. Properly trained learning-based methods tend to generalize well even when the signal-to-noise ratio (SNR) is low or in highly reverberant environments [108].

With deep learning methods emerging, an increasing number of works tackle the problem of sound source localization by training an audio network, which aims to find the relationship between the input audio features and the positions of the sound sources. Compared to traditional parametric-based methods, the learning-based methods are more robust and generalize better in the presence of reverberation and acoustic noise. Neural networks were employed in [106] to predict the 3D positions of speakers given multi-channel audio signals recorded by microphone arrays. A DeepGCC was designed in [109] that can estimate sound source positions robustly in different environments with various room geometry and microphone array configurations. A convolutional recurrent neural network (CRNN) was used in [110] to detect and localize sound events concurrently. CRNN has been widely employed to localize moving sounds [111], and with different audio input features [112]–[114]. In [20], a two-stage strategy was used where sound event detection is conducted first, and then the predicted event is used to assist the localization of sound sources. In [115], a sequence-to-sequence model with an attention mechanism was designed to predict DOA. In [116], Transformer [117] is used for localizing sound sources.

The audio features Mel-spectrogram, the mel frequency cepstral coefficients (MFCC), and GCC-PHAT are often selected as the input. Nguyen et al. [118] recently proposed the Spatial Cue-Augmented Log-Spectrogram (SALSA) features. They consist of a normalized version of the principal eigenvector of the spatial covariance matrix computed at each time-frequency bin. This enables concatenation with the spectrograms extracted from the microphone array's channels. Subsequently, the authors proposed SALSA-Lite [119], a lighter version consisting of the frequency-normalized interchannel phase difference (IPD) computed at each time-frequency bin. These features have shown promising performance on task 3 of the Challenge on Detection and Classification of Acoustic Scenes and Events (DCASE): sound event detection and localization.

3) Extracting Features in Teacher-Student Paradigm

Learning-based sound source localization methods typically require extensive amounts of annotated training data. However, in the task of audio-visual speaker tracking, acquiring such data is often challenging. For example, as summarized in [85], AV16.3 [120] contains 5-minute annotated sequences

and CAV3D [12] contains 14-minute annotated sequences, which is not sufficient for training. One possible solution to the problem of insufficient data is the teacher-student paradigm, also referred to as knowledge distillation [121]. It adopts a network pre-trained on the desired task (teacher) to automatically extract pseudo-labels from an unlabelled dataset. The pseudo-labels are then used to supervise the training of a new network (student), trained to produce the same results. The student networks are always more light-weighted than the teacher networks. In audio-visual learning, typically one modality is used to supervise its counterpart. Under the guidance of visual modality, audio can be used for complicated tasks [122], including semantic segmentation [123], depth perception [124], acoustic scene classification [125], speaker detection and localization [107], [122] and vehicle localization [126] [127]. In these works a visual teacher network is used to extract positional pseudo-labels to train a multi-channel audio student network. The visual modality can provide beneficial supervision for audio as it has higher spatial accuracy, using color histograms or face detection. In contrast, the audio modality is omnidirectional, presents higher temporal resolution, and does not fail when the speaker is visually occluded.

C. Audio-Visual Fusion

The methods for audio-visual fusion can be classified into three types: early fusion, late fusion and intermediate fusion [128].

Early fusion methods combine the audio and visual features before the Bayesian inference. Few works use this method as the feature representation between the audio and visual modalities is inherently different and combining the heterogeneous information at an early stage is a challenging problem. In [13], GCC-PHAT and simulated visual features are encoded concurrently to predict DOA estimations.

Late fusion makes the final decision by combining the decisions from an audio tracker and a visual tracker. There are several works using late fusion. Kalman filter was used in [40] to process audio and visual signals separately, and then Gaussian distribution is used and fused to get the object states. In [77], GCF and face detectors were used to get two estimated positions, and PF was employed to fuse the two decisions.

Intermediate fusion allows the audio and visual signals to interact with each other before making decisions and is the most widely used fusion method. In [12], the height estimation by visual modality was employed to assist the GCF calculation. In [80], two particle filters were used to process audio and visual streams independently, and the confidence of audio and visual modalities is leveraged to dynamically adjust the weights of particles. In [89], a multi-modal perception attention network was proposed with a self-supervised cross-modal strategy to determine the importance of audio and visual measurements. In [129], binaural audios and visual frames are encoded separately and fused

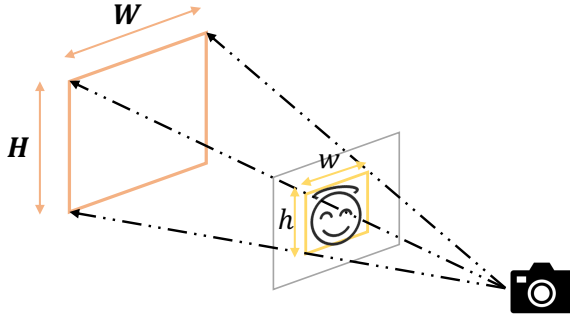


FIGURE 5. The Camera Projection Model

through ConvLSTM before the decoder for sound source localization.

D. Position Conversion between 2D and 3D

The 2D position in the image plane and the 3D position in the world coordinates can be converted to each other through the camera projection model [102], as shown in Figure 5. The 2D position \mathbf{o} derived by face detection can be converted to 3D position \mathbf{O} :

$$\mathbf{O} = \Phi(\mathbf{o}; w, h, W, H) \quad (26)$$

where (w, h) is the width and height of the face bounding boxes. (W, H) is the preset width and height of the face bounding box in the 3D space.

Similarly, the 3D position obtained by the sound source localization algorithm can be converted to a 2D position:

$$\mathbf{o} = \Psi(\mathbf{O}; W, H) \quad (27)$$

E. Data Association

In the scenario of multiple speaker tracking and single target tracking with clutter and false alarms, data association is needed, which contains two aspects of audio-visual speaker tracking. The one is to associate audio measurements with corresponding visual measurements for audio-visual fusion, which will be discussed in Section C. The other is to associate the fused measurements to the existing tracks, clutter and the new tracks.

The Nearest Neighbor (NN) algorithm is the simplest data association method, which associates the closest measurements with the target. NN regards the data association as linear programming and minimizes the association cost globally. While NN is easy to associate clutter or false alarms with targets and deviates from the tracks. JPDA [130] is short for Joint Probabilistic Data Association, which assumes that each measurement originates from clutter or targets and each target can only generate one measurement. Each target may have multiple effective measurements. JPDA calculates the joint probability of targets associated with different effective measurements. The drawback of JPDA is that it requires the prior of the number of targets and fails in the scenario of missing targets. MHT [131] (Multiple

Hypothesis Tracking) maintains an association hypothesis tree and calculates possibilities of all association hypothesis branches. A new measurement can be associated with an old hypothesis, can start a new hypothesis and can be a false alarm. The computational cost of MHT is increasing exponentially with the number of measurements. To lower the computational cost, the hypothesis with low possibility can be deleted and similar hypotheses can be merged.

V. Datasets

Most datasets for audio-visual speaker tracking are recorded by microphone arrays and cameras. The microphone array can be circular, planar, T-shaped or in other shapes. The audio-visual datasets can be classified as co-located or spatially distributed depending on whether the multi-modal sensors are co-located or not. Most datasets provide the recording timing sequences used to synchronize the multi-modal sequences. The annotations contain the camera calibration information, voice activity detectors and ground truth positions. Camera calibration information is usually used to project 2D coordinates to 3D coordinates or project in reverse [102]. Voice activity detectors denote whether the speakers are talking over frames. Ground truth positions are often the face bounding boxes and mouth positions. In [12], some audio-visual datasets were summarized for speaker tracking. We give a more thorough review of the commonly used datasets in Table 8. In addition to the audio-visual speakers tracking datasets, we also list some multi-modal datasets for objects such as vehicle [127] and small objects [94]. Besides, datasets containing other modalities such as depth [140] and thermal maps [127] are included. We also introduce some influential datasets in detail.

A. AV16.3 Dataset

AV16.3 [120] dataset is widely employed for evaluating speaker localization and tracking systems. AV16.3 dataset was captured using two circular microphone arrays and three cameras. For audio, each microphone array has 8 microphones arranged in a circular geometry, recording at a 16 kHz sampling rate. For video, three synchronized cameras capture images at 25 frames per second. The two microphone arrays are located 0.8 meters apart at a table. Within the AV16.3 dataset, speakers in the recording space engage in various activities, including sitting statically, standing statically, or walking near the table. The duration of most sequences range from 20 to 60 seconds, although there are also longer sequences that extend beyond three minutes. AV16.3 dataset contains over 40 different audio-visual sequences. However, only a small subset of these sequences have annotated ground truth labels. Sequences 08, 11, 12, 19 and 20 are often used for the evaluation of single-speaker tracking while sequences 24, 25 and 30 are often used for the evaluation of multiple-speaker tracking. These particular sequences are challenging due to occurrences of occlusions

TABLE 8. Multi-modal Datasets. No. Mic denotes the number of microphones over all microphone arrays; SR denotes the sampling rate with the unit of kHz; CA (Circular microphone Arrays) denotes whether the microphone array is in the circular shape; No. Cam denotes the number of cameras; Fps denotes frame per second; Co (Co-located) denotes whether the multi-modal sensors are co-located; Cal (Calibration information) denotes whether the camera calibration information is available; VAD (Voice activity Detectors) denotes whether the speakers’ states are available; Type denotes the formats of the annotation; No. Spk denotes the maximum number of speakers in one frame and ‘-’ denotes ‘not applicable’.

Dataset	Audio			Video			Co	Annotation			No. Spk
	No. Mic	SR (kHz)	CA	No. Cam	Resolution (pixels)	Fps		Cal	VAD	Type	
AVTRACK-1 [132]	4	44.1	-	2	640 × 480	25	✓	-	✓	Active speaker(s) bounding box, upper-body region bounding box	2
AVASM [133]	2	44.1	-	2	640 × 480	-	✓	-	-	2D coordinates of a loud-speaker	2
AVDIAR [3]	6	48	-	2	1920 × 1200	25	✓	✓	✓	2D coordinates of the head and upper-body	4
RAVEL [134]	4	48	-	2	1024 × 768	15	✓	✓	✓	Both 2D and 3D coordinates of actors’ positions	5
CAVA [135]	2	44.1	-	2	1024 × 768	25	✓	✓	-	3D trajectory of head tracking	5
SPEVI [136]	2	44.1	-	1	360 × 288	25	✓	-	-	Face bound boxes	2
AMI [137]	-	48	✓	-	720 × 576	25	-	-	✓	Occlusion status, head, hand and face positions	4
CHIL [138]	88	44.1	-	5	1024 × 768	30	-	✓	✓	Face, head, eyes and nose positions	5
AV16.3 [120]	16	16	✓	3	360 × 288	25	-	✓	✓	Both 2D and 3D face and head positions	3
CAV3D [12]	8	96	✓	1	1024 × 768	15	✓	✓	✓	Mouth positions	3
CLEAR [139]	14+	44.1	-	4	1024 × 768	30	✓	✓	✓	Both 2D and 3D head locations, face bound boxes	8
S3A [140]	2	44.1	-	1	-	30	-	-	-	No visual information is provided but depth information is provided	-
TragicTalkers [141]	38	48	-	22	2448 × 2048	30	✓	✓	✓	3D mouth positions and pseudo labels	2
AVOT [94]	-	44.1	-	-	800 × 600	-	-	-	-	2D positions of tabletoped sized objects	-
SSLR [142]	4	48	-	-	-	-	-	-	✓	3D positions of sound sources	2
MAVD [127]	8	44.1	✓	2	1920 × 650	-	✓	-	-	No ground truth available. In addition to audio and visual modalities, thermal and depth modalities are also provided	-
AVIAD [143]	128	12	-	1	640 × 480	-	✓	-	-	People’s actions	1
AVRI [63]	4	-	-	1	960 × 540	-	✓	-	-	Azimuth (Direction of Arrival)	1
EasyCom [144]	4+	48	✓	1	1920 × 1080	20	✓	✓	✓	3D positions and rotations	1

and instances where speakers are not facing the cameras, adding complexity to the tracking evaluation process.

B. CAV3D Dataset

CAV3D is a dataset recorded by Co-located Audio-Visual sensors for 3D tracking. It is recorded in a $4.66 \times 5.95 \times 4.5$ room with an eight-microphone circular array with a sample rate of 96kHz and a camera with 25 fps. This dataset contains nine single-speaker sequences and 11 multiple-speaker

sequences. Compared to the AV16.3 dataset, scenarios in the CAV3D dataset are more challenging as it contains more frames where speakers are occluded by each other and speakers are outside the field of view of the camera.

C. AVRI Dataset

Different from the previous dataset, AVRI (Audio-Visual Robotic Interface) has around 9 hours, which provides sufficient data for training a neural network. ReSpeaker

microphone array is used to record the multi-channel audio with 16kHz and a Kinect sensor is used for RGB capture with 960×540 resolution. OptiTrack system is used to annotate the recorded sequence and provide 3D ground truth.

VI. Metrics

There are several metrics to evaluate the performance of audio-visual speaker trackers such as OSPA [145], MAE, TLR, MOTA [146] and MOTP [146].

A. OSPA

Optimal Sub-Pattern Assignment (OSPA), as defined in [145], operates on the reference set $M = \{m_1, m_2, \dots, m_{|M|}\}$ and the estimated set $N = \{n_1, n_2, \dots, n_{|N|}\}$. Here, $|\cdot|$ represents the length of each set.

$$E_\rho^{(c)}(M, N) = \left(\frac{1}{|N|} \left(\min_{\pi \in \Pi_{|N|}} \sum_{i=1}^{|M|} d^{(c)}(m_i, n_{\pi(i)})^\rho + c^\rho (|N| - |M|) \right) \right)^{\frac{1}{\rho}} \quad (28)$$

where $c > 0$ defines the largest distance and accounts for the cardinality errors, and $\rho \geq 1$ is the order. $\Pi_{|N|}$ denotes the set of permutations on $\{1, 2, \dots, |N|\}$. The term $d^{(c)}(m_i, n_{\pi(i)})$ is the minimum between $(\|m_i - n_{\pi(i)}\|_2)$ and c .

The objective of this metric is to determine the optimal assignment of points within sets M and N , effectively associating them while calculating the ρ -order distance between the matched points. Points within set N that remain unassociated contribute to cardinality errors.

B. MAE

MAE stands for Mean Absolute Error, defined as follows:

$$\varepsilon = \frac{1}{|K|T} \sum_{i=1}^{|K|} \sum_{t=1}^T \|\hat{\mathbf{x}}_{t,i} - \mathbf{x}_{t,i}\|_2 \quad (29)$$

where $|K|$ is the number of targets, T is the number of time frames, $\hat{\mathbf{x}}_{t,i}$ is the predicted position and $\mathbf{x}_{t,i}$ is the ground truth position.

C. TLR

TLR is the Track Loss Rate, defined as the percentage of unsuccessful tracking over all frames. For 2D tracking on the image plane, the unsuccessful tracking is defined as that MAE is beyond $1/\lambda_{2D}$ of the length of the image diagonal. For 3D tracking, the unsuccessful tracking is defined as the case where the MAE is beyond λ_{3D} centimeters. Typically, λ_{2D} is often set as 15 and λ_{3D} is often set as 30 cm.

D. MOTA

MOTA is the multiple object tracking accuracy, which is defined as follows:

$$\text{MOTA} = 100\% \times \left(1 - \frac{\sum_t (\text{FN}_t + \text{FP}_t + \text{MM}_t)}{\sum_t G_t} \right) \quad (30)$$

where FN is the number of false negative targets, or the missing targets, FP is the number of false positive targets, MM is the number of mismatches, and G is the number of ground truth targets.

E. MOTP

MOTP stands for the multiple object tracking precision and is defined as the average localization errors over matched targets:

$$\text{MOTP} = \frac{\sum_{i,t} e_t^i}{\sum_t m_t} \quad (31)$$

where e_t^i is the Euclidean distance between the i -th predicted target and the matched ground truth, and m_t is the number of matched pairs at time step t .

In addition to the aforementioned metrics, other metrics such as higher order tracking accuracy (HOTA) [147], most tracked targets (MT) and most lost targets (ML) are also used. The details can be found in the MOT Challenge¹.

F. Metrics for Measuring Computational Efficiency

The metrics mentioned above are performance metrics. The computation time of trackers is also important as some applications have real-time requirements [54]. For evaluating the tracker's processing velocity, Frame per Second (FPS) is a good choice. Floating Point Operations Per Second (FLOPS) can also be used.

VII. Future Directions

A. Audio-Visual Multiple Speaker Tracking with Speech Separation

Audio-visual tracking can assist speech separation. Compared to the deep learning based methods such as [148] and [149], the detection, tracking and filtering (DTF) framework for speech separation can be adapted to the varying numbers of speakers without training on large-scale datasets. In [150], GLMB is employed to generate speaker trajectories with audio and visual measurements. The generalized side-lobe canceller (GSC) [151] is implemented based on the trajectories to perform online speech separation. In [152], an end-to-end far-field speech recognition system is proposed integrating localization, separation and ASR. The localization part gives the interpretation and improves the performance.

Speech separation can help the obtaining of the audio measurements. In [153], deep neural networks are used to calculate time-frequency masking, aiming to obtain the clean phase for DOA estimation. In [154], the speech separation method is used for DOA estimation. And the obtained DOA improves the performance of downstream tasks such as ASR. In [155], voicefilter [149] is used to separate the target voice before localizing the target speaker.

¹<https://motchallenge.net/results/MOT15/>

B. Audio-Visual Multiple Speaker Tracking in Distributed Scenarios

Audio-visual tracking utilizes more modalities to improve tracking accuracy than past tracking systems, which use a single modality. However, most of the existing works for audio-visual tracking only utilize one microphone array and one camera, and those sensors are often regarded as one node. Therefore, when a sensor in the node cannot work as well as expected, the unreliable measurements from that sensor will degrade the tracking accuracy. The simple idea for solving this problem is to increase the number of nodes to obtain global estimates, which can mitigate the impacts of errors in each node's estimates. Thus, there has been a growing interest in the development of tracking systems using distributed sensors, which have the potential to enhance tracking accuracy and reliability [156]. Recently, several distributed filters have been proposed for tracking in the distributed scenario [157]–[160].

C. Audio-Visual Multiple Speaker Tracking in Egocentric Scenarios

Recently tasks in egocentric scenarios arise increasing interest as the egocentric scenario mimics the similar way as humans explore the world. There are some large-scale datasets such as Epic-kitchen [161] and Ego4D [162] for egocentric perception. In these datasets, one person wears egocentric equipment (the wearer) such as cameras and microphones to record their daily life. Audio-visual speaker tracking in egocentric scenarios is beneficial for audio-visual navigation and human robot interaction. However, there are some challenges, which differ from the conventional audio-visual speaker tracking scenarios, including motion blur, speaker disappearance due to the movement of the wearer and occlusions. For this task, the Easycom dataset [144] is proposed for audio-visual active speaker localization and tracking in the egocentric scenario. In [163], a simulated is proposed, in which the speaker moves more frequently and more out-of-view scenarios are included compared to the Easycom dataset.

D. Prompt-Based Target Speaker Tracking

Text and audio signals can be used as prompts to describe the target sound event. Text prompt is used in [164] for target object tracking. In [165], target speech diarization is proposed and text can be used to indicate the target speaker such as the female speaker or the dominant speaker. Audio prompt is used in [155] to provide reference speech for target speaker localization. For the task of audio-visual speaker tracking, audio or text prompts can be used to describe the target speaker as well. The prompt-based tracking task provides a more user-friendly way of human-computer interaction and can be used in monitoring systems.

VIII. Conclusions

In this paper, we conduct a comprehensive literature review on audio-visual speaker tracking. We recall the existing methods for obtaining audio and visual measurements. And we introduce the Bayesian filters. We discuss the new techniques, especially the deep learning based methods such as the learning-based features and differentiable Bayesian filters. Though the development of audio-visual speaker tracking has been progressive during the past few years, there remain some problems. Firstly, most current trackers do not evaluate the computational complexities. However, some downstream tasks such as speech enhancement and monitoring have the requirements of real-time tracking. In addition, there still a lack of large-scale datasets for audio-visual multiple speakers tracking, for which deep learning techniques are not fully explored in this traditional task.

IX. Author Contributions

Jinzheng Zhao: Writing – original draft. **Yong Xu:** Project administration; Review and editing. **Xinyuan Qian:** Review and editing. **Davide Berghi:** Writing - Part of contents in Section I and Section IV.B.3. **Peipei Wu:** Writing - Section VII.B. **Meng Cui:** Discussion. **Jianyuan Sun:** Discussion. **Philip J.B. Jackson:** Discussion and analysis. **Wenwu Wang:** Project administration; Review and editing. Funding acquisition.

REFERENCES

- [1] S. T. Shivappa, B. D. Rao, and M. M. Trivedi, "Audio-visual fusion and tracking with multilevel iterative decoding: Framework and experimental evaluation," *IEEE Journal of Selected Topics in Signal Processing*, vol. 4, no. 5, pp. 882–894, 2010.
- [2] G. Potamianos, C. Neti, and S. Deligne, "Joint audio-visual speech processing for recognition and enhancement," in *AVSP 2003-International Conference on Audio-Visual Speech Processing*, 2003.
- [3] I. D. Gebru, S. Ba, X. Li, and R. Horaud, "Audio-visual speaker diarization based on spatiotemporal bayesian fusion," *IEEE transactions on pattern analysis and machine intelligence*, vol. 40, no. 5, pp. 1086–1099, 2017.
- [4] P. C. Loizou, *Speech Enhancement: Theory and Practice*. CRC Press, 2007.
- [5] A. Hampapur, L. Brown, J. Connell, A. Ekin, N. Haas, M. Lu, H. Merkl, and S. Pankanti, "Smart video surveillance: exploring the concept of multiscale spatiotemporal tracking," *IEEE signal processing magazine*, vol. 22, no. 2, pp. 38–51, 2005.
- [6] C. Pike, R. Taylor, T. Parnell, and F. Melchior, "Object-based 3d audio production for virtual reality using the audio definition model," *AES International Conference on Audio for Virtual and Augmented Reality*, September 2016.
- [7] P. Coleman, A. Franck, J. Francombe, Q. Liu, T. de Campos, R. J. Hughes, D. Menzies, M. F. S. Gálvez, Y. Tang, J. Woodcock, P. J. B. Jackson, F. Melchior, C. Pike, F. M. Fazi, T. J. Cox, and A. Hilton, "An audio-visual system for object-based audio: From recording to listening," *IEEE Transactions on Multimedia*, vol. 20, no. 8, pp. 1919–1931, 2018.
- [8] M. A. Mohd Izhar, M. Volino, A. Hilton, and P. J. B. Jackson, "Tracking sound sources for object-based spatial audio in 3D audio-visual production," in *Forum Acusticum*, pp. 2051–2058, 2020.
- [9] F. Schweiger, C. Pike, T. Nixon, M. Firth, B. Weir, P. Golds, M. Volino, C. Cieciora, M. Izhar, N. Graham-Rack, P. J. B. Jackson, and A. Ang, "Tools for 6-dof immersive audio-visual content capture and production," in *IBC*, 2022.
- [10] J. Zhao, P. Wu, X. Liu, Y. Xu, L. Mihaylova, S. Godsill, and W. Wang, "Audio-visual tracking of multiple speakers via a pmbm filter," in

- Proceedings of the IEEE International Conference on Acoustics, Speech, and Signal Processing (ICASSP)*, IEEE, 2022.
- [11] V. Kılıç and W. Wang, "Audio-visual speaker tracking," in *Motion Tracking and Gesture Recognition*, IntechOpen, 2017.
 - [12] X. Qian, A. Brutti, O. Lanz, M. Omologo, and A. Cavallaro, "Multi-speaker tracking from an audio-visual sensing device," *IEEE Transactions on Multimedia*, vol. 21, no. 10, pp. 2576–2588, 2019.
 - [13] X. Qian, M. Madhavi, Z. Pan, J. Wang, and H. Li, "Multi-target doa estimation with an audio-visual fusion mechanism," in *ICASSP 2021-2021 IEEE International Conference on Acoustics, Speech and Signal Processing (ICASSP)*, pp. 4280–4284, IEEE, 2021.
 - [14] S. T. Birchfield and S. Rangarajan, "Spatiograms versus histograms for region-based tracking," in *2005 IEEE Computer Society Conference on Computer Vision and Pattern Recognition (CVPR'05)*, vol. 2, pp. 1158–1163, IEEE, 2005.
 - [15] T. Ojala, M. Pietikainen, and T. Maenpää, "Multiresolution gray-scale and rotation invariant texture classification with local binary patterns," *IEEE Transactions on pattern analysis and machine intelligence*, vol. 24, no. 7, pp. 971–987, 2002.
 - [16] D. G. Lowe, "Distinctive image features from scale-invariant keypoints," *International journal of computer vision*, vol. 60, no. 2, pp. 91–110, 2004.
 - [17] M. Omologo, P. Svaizer, and R. DeMori, "Spoken dialogue with computers," 1998.
 - [18] G. Lathoud and M. Magimai-Doss, "A sector-based, frequency-domain approach to detection and localization of multiple speakers," in *Proceedings (ICASSP'05). IEEE International Conference on Acoustics, Speech, and Signal Processing, 2005.*, vol. 3, pp. iii–265, IEEE, 2005.
 - [19] R. Schmidt, "Multiple emitter location and signal parameter estimation," *IEEE transactions on antennas and propagation*, vol. 34, no. 3, pp. 276–280, 1986.
 - [20] Y. Cao, Q. Kong, T. Iqbal, F. An, W. Wang, and M. D. Plumbley, "Polyphonic sound event detection and localization using a two-stage strategy," *arXiv preprint arXiv:1905.00268*, 2019.
 - [21] R. E. Kalman, "A new approach to linear filtering and prediction problems," 1960.
 - [22] M. S. Arulampalam, S. Maskell, N. Gordon, and T. Clapp, "A tutorial on particle filters for online nonlinear/non-gaussian bayesian tracking," *IEEE Transactions on signal processing*, vol. 50, no. 2, pp. 174–188, 2002.
 - [23] R. P. S. Mahler, *Statistical Multisource-Multitarget Information Fusion*. USA: Artech House, Inc., 2007.
 - [24] R. P. Mahler, "Multitarget bayes filtering via first-order multitarget moments," *IEEE Transactions on Aerospace and Electronic systems*, vol. 39, no. 4, pp. 1152–1178, 2003.
 - [25] R. P. Mahler, *Statistical multisource-multitarget information fusion*, vol. 685. Artech House Norwood, MA, USA, 2007.
 - [26] B.-T. Vo, B.-N. Vo, and A. Cantoni, "The cardinality balanced multi-target multi-bernoulli filter and its implementations," *IEEE Transactions on Signal Processing*, vol. 57, no. 2, pp. 409–423, 2008.
 - [27] B.-T. Vo and B.-N. Vo, "Labeled random finite sets and multi-object conjugate priors," *IEEE Transactions on Signal Processing*, vol. 61, no. 13, pp. 3460–3475, 2013.
 - [28] J. L. Williams, "Marginal multi-bernoulli filters: Rfs derivation of mht, jipda, and association-based member," *IEEE Transactions on Aerospace and Electronic Systems*, vol. 51, no. 3, pp. 1664–1687, 2015.
 - [29] Á. F. García-Fernández, J. L. Williams, K. Granström, and L. Svensson, "Poisson multi-bernoulli mixture filter: direct derivation and implementation," *IEEE Transactions on Aerospace and Electronic Systems*, vol. 54, no. 4, pp. 1883–1901, 2018.
 - [30] Y. Xia, K. Granstrom, L. Svensson, and Á. F. García-Fernández, "Performance evaluation of multi-bernoulli conjugate priors for multi-target filtering," in *2017 20th International Conference on Information Fusion (Fusion)*, pp. 1–8, IEEE, 2017.
 - [31] S. Scheidegger, J. Benjaminsson, E. Rosenberg, A. Krishnan, and K. Granström, "Mono-camera 3d multi-object tracking using deep learning detections and pmbm filtering," in *2018 IEEE Intelligent Vehicles Symposium (IV)*, pp. 433–440, IEEE, 2018.
 - [32] S. Pang and H. Radha, "Multi-object tracking using poisson multi-bernoulli mixture filtering for autonomous vehicles," in *IEEE International Conference on Acoustics, Speech and Signal Processing (ICASSP)*, pp. 7963–7967, IEEE, 2021.
 - [33] C. Schymura and D. Kolossa, "Audiovisual speaker tracking using nonlinear dynamical systems with dynamic stream weights," *IEEE/ACM Transactions on Audio, Speech, and Language Processing*, vol. 28, pp. 1065–1078, 2020.
 - [34] C. Schymura, T. Ochiai, M. Delcroix, K. Kinoshita, T. Nakatani, S. Araki, and D. Kolossa, "A dynamic stream weight backprop kalman filter for audiovisual speaker tracking," in *ICASSP 2020-2020 IEEE International Conference on Acoustics, Speech and Signal Processing (ICASSP)*, pp. 581–585, IEEE, 2020.
 - [35] A. Bewley, Z. Ge, L. Ott, F. Ramos, and B. Upcroft, "Simple online and realtime tracking," in *2016 IEEE international conference on image processing (ICIP)*, pp. 3464–3468, IEEE, 2016.
 - [36] H. W. Kuhn, "The hungarian method for the assignment problem," *Naval research logistics quarterly*, vol. 2, no. 1-2, pp. 83–97, 1955.
 - [37] N. Wojke, A. Bewley, and D. Paulus, "Simple online and realtime tracking with a deep association metric," in *2017 IEEE international conference on image processing (ICIP)*, pp. 3645–3649, IEEE, 2017.
 - [38] D. Simon, *Optimal state estimation: Kalman, H infinity, and nonlinear approaches*. John Wiley & Sons, 2006.
 - [39] E. A. Wan, R. Van Der Merwe, and S. Haykin, "The unscented kalman filter," *Kalman filtering and neural networks*, vol. 5, no. 2007, pp. 221–280, 2001.
 - [40] E. D'Arca, N. M. Robertson, and J. Hopgood, "Person tracking via audio and video fusion," 2012.
 - [41] J. S. Liu and R. Chen, "Sequential monte carlo methods for dynamic systems," *Journal of the American statistical association*, vol. 93, no. 443, pp. 1032–1044, 1998.
 - [42] G. Kitagawa, "Monte carlo filter and smoother for non-gaussian nonlinear state space models," *Journal of computational and graphical statistics*, vol. 5, no. 1, pp. 1–25, 1996.
 - [43] Z. Fang, G. Tong, and X. Xu, "Particle swarm optimized particle filter," *Control and decision*, vol. 22, no. 3, p. 273, 2007.
 - [44] M. Tian, Y. Bo, Z. Chen, P. Wu, and C. Yue, "A new improved firefly clustering algorithm for smc-phd filter," *Applied Soft Computing*, vol. 85, p. 105840, 2019.
 - [45] M. Tian, Z. Chen, H. Wang, and L. Liu, "An intelligent particle filter for infrared dim small target detection and tracking," *IEEE Transactions on Aerospace and Electronic Systems*, 2022.
 - [46] B.-N. Vo and W.-K. Ma, "The gaussian mixture probability hypothesis density filter," *IEEE Transactions on signal processing*, vol. 54, no. 11, pp. 4091–4104, 2006.
 - [47] B.-N. Vo, S. Singh, and A. Doucet, "Sequential monte carlo methods for multitarget filtering with random finite sets," *IEEE Transactions on Aerospace and electronic systems*, vol. 41, no. 4, pp. 1224–1245, 2005.
 - [48] Y. Liu, W. Wang, J. Chambers, V. Kilic, and A. Hilton, "Particle flow smc-phd filter for audio-visual multi-speaker tracking," in *International Conference on Latent Variable Analysis and Signal Separation*, pp. 344–353, Springer, 2017.
 - [49] F. Daum and J. Huang, "Nonlinear filters with log-homotopy," in *Signal and Data Processing of Small Targets 2007*, vol. 6699, pp. 423–437, SPIE, 2007.
 - [50] Y. Ban, X. Alameda-Pineda, L. Girin, and R. Horaud, "Variational bayesian inference for audio-visual tracking of multiple speakers," *IEEE transactions on pattern analysis and machine intelligence*, vol. 43, no. 5, pp. 1761–1776, 2019.
 - [51] W. Zhang, H. Zhou, S. Sun, Z. Wang, J. Shi, and C. C. Loy, "Robust multi-modality multi-object tracking," in *Proceedings of the IEEE/CVF International Conference on Computer Vision*, pp. 2365–2374, 2019.
 - [52] A. Geiger, P. Lenz, and R. Urtasun, "Are we ready for autonomous driving? the kitti vision benchmark suite," in *2012 IEEE conference on computer vision and pattern recognition*, pp. 3354–3361, IEEE, 2012.
 - [53] P. Ondruska and I. Posner, "Deep tracking: Seeing beyond seeing using recurrent neural networks," in *Thirtieth AAAI conference on artificial intelligence*, 2016.
 - [54] A. Milan, S. H. Rezatofighi, A. Dick, I. Reid, and K. Schindler, "Online multi-target tracking using recurrent neural networks," in *Thirty-First AAAI conference on artificial intelligence*, 2017.
 - [55] T. Meinhardt, A. Kirillov, L. Leal-Taixe, and C. Feichtenhofer, "Trackformer: Multi-object tracking with transformers," in *Proceedings of the IEEE/CVF conference on computer vision and pattern recognition*, pp. 8844–8854, 2022.

- [56] P. Sun, J. Cao, Y. Jiang, R. Zhang, E. Xie, Z. Yuan, C. Wang, and P. Luo, "Transtrack: Multiple object tracking with transformer," *arXiv preprint arXiv:2012.15460*, 2020.
- [57] Y. Zhang, P. Sun, Y. Jiang, D. Yu, F. Weng, Z. Yuan, P. Luo, W. Liu, and X. Wang, "Bytetrack: Multi-object tracking by associating every detection box," in *European Conference on Computer Vision*, pp. 1–21, Springer, 2022.
- [58] Z. Qin, S. Zhou, L. Wang, J. Duan, G. Hua, and W. Tang, "Motion-track: Learning robust short-term and long-term motions for multi-object tracking," in *Proceedings of the IEEE/CVF Conference on Computer Vision and Pattern Recognition*, pp. 17939–17948, 2023.
- [59] Y. Xu, X. Zhou, S. Chen, and F. Li, "Deep learning for multiple object tracking: a survey," *IET Computer Vision*, vol. 13, no. 4, pp. 355–368, 2019.
- [60] G. Wang, M. Song, and J.-N. Hwang, "Recent advances in embedding methods for multi-object tracking: a survey," *arXiv preprint arXiv:2205.10766*, 2022.
- [61] J. Willes, C. Reading, and S. L. Waslander, "Intertrack: Interaction transformer for 3d multi-object tracking," in *2023 20th Conference on Robots and Vision (CRV)*, pp. 73–80, IEEE, 2023.
- [62] X. Geng, M. Li, W. Liu, S. Zhu, H. Jiang, J. Bian, X. Fan, R. Peng, and J. Luo, "Person tracking by detection using dual visible-infrared cameras," *IEEE Internet of Things Journal*, vol. 9, no. 22, pp. 23241–23251, 2022.
- [63] X. Qian, Z. Wang, J. Wang, G. Guan, and H. Li, "Audio-visual cross-attention network for robotic speaker tracking," *IEEE/ACM Transactions on Audio, Speech, and Language Processing*, vol. 31, pp. 550–562, 2022.
- [64] T. Haarnoja, A. Ajay, S. Levine, and P. Abbeel, "Backprop kf: Learning discriminative deterministic state estimators," *Advances in neural information processing systems*, vol. 29, 2016.
- [65] S. Kim, I. Petrunin, and H.-S. Shin, "A review of kalman filter with artificial intelligence techniques," in *2022 Integrated Communication, Navigation and Surveillance Conference (ICNS)*, pp. 1–12, IEEE, 2022.
- [66] R. Jonschkowski, D. Rastogi, and O. Brock, "Differentiable particle filters: End-to-end learning with algorithmic priors," *arXiv preprint arXiv:1805.11122*, 2018.
- [67] A. Geiger, P. Lenz, C. Stiller, and R. Urtasun, "Vision meets robotics: The kitti dataset," *The International Journal of Robotics Research*, vol. 32, no. 11, pp. 1231–1237, 2013.
- [68] P. Karkus, D. Hsu, and W. S. Lee, "Particle filter networks with application to visual localization," in *Conference on robot learning*, pp. 169–178, PMLR, 2018.
- [69] M. Zhu, K. Murphy, and R. Jonschkowski, "Towards differentiable resampling," *arXiv preprint arXiv:2004.11938*, 2020.
- [70] X. Ma, P. Karkus, D. Hsu, and W. S. Lee, "Particle filter recurrent neural networks," in *Proceedings of the AAAI Conference on Artificial Intelligence*, vol. 34, pp. 5101–5108, 2020.
- [71] Y. Zhang, M. Yu, H. Zhang, D. Yu, and D. Wang, "Kalmannet: A learnable kalman filter for acoustic echo cancellation," *arXiv preprint arXiv:2301.12363*, 2023.
- [72] S. Jouaber, S. Bonnabel, S. Velasco-Forero, and M. Pilte, "Nnakf: A neural network adapted kalman filter for target tracking," in *ICASSP 2021-2021 IEEE International Conference on Acoustics, Speech and Signal Processing (ICASSP)*, pp. 4075–4079, IEEE, 2021.
- [73] J. Zhao, M. Plumbley, W. Wang, *et al.*, "Attention-based end-to-end differentiable particle filter for audio speaker tracking," 2023.
- [74] M. Barnard, P. Koniusz, W. Wang, J. Kittler, S. M. Naqvi, and J. Chambers, "Robust multi-speaker tracking via dictionary learning and identity modeling," *IEEE Transactions on Multimedia*, vol. 16, no. 3, pp. 864–880, 2014.
- [75] V. Kılıç, M. Barnard, W. Wang, and J. Kittler, "Audio assisted robust visual tracking with adaptive particle filtering," *IEEE Transactions on Multimedia*, vol. 17, no. 2, pp. 186–200, 2014.
- [76] V. Kılıç, M. Barnard, W. Wang, A. Hilton, and J. Kittler, "Mean-shift and sparse sampling-based smc-phd filtering for audio informed visual speaker tracking," *IEEE Transactions on Multimedia*, vol. 18, no. 12, pp. 2417–2431, 2016.
- [77] X. Qian, A. Brutti, M. Omologo, and A. Cavallaro, "3d audio-visual speaker tracking with an adaptive particle filter," in *2017 IEEE International Conference on Acoustics, Speech and Signal Processing (ICASSP)*, pp. 2896–2900, IEEE, 2017.
- [78] X. Qian, A. Xompero, A. Cavallaro, A. Brutti, O. Lanz, and M. Omologo, "3d mouth tracking from a compact microphone array co-located with a camera," in *2018 IEEE International Conference on Acoustics, Speech and Signal Processing (ICASSP)*, pp. 3071–3075, IEEE, 2018.
- [79] Y. Liu, V. Kılıç, J. Guan, and W. Wang, "Audio-visual particle flow smc-phd filtering for multi-speaker tracking," *IEEE Transactions on Multimedia*, vol. 22, no. 4, pp. 934–948, 2019.
- [80] H. Liu, Y. Li, and B. Yang, "3d audio-visual speaker tracking with a two-layer particle filter," in *2019 IEEE International Conference on Image Processing (ICIP)*, pp. 1955–1959, IEEE, 2019.
- [81] S. Lin and X. Qian, "Audio-visual multi-speaker tracking based on the glmb framework," in *INTERSPEECH*, pp. 3082–3086, 2020.
- [82] H. Liu, Y. Sun, Y. Li, and B. Yang, "3d audio-visual speaker tracking with a novel particle filter," in *2020 25th International Conference on Pattern Recognition (ICPR)*, pp. 7343–7348, IEEE, 2021.
- [83] Y. Li, H. Liu, and H. Tang, "Multi-modal perception attention network with self-supervised learning for audio-visual speaker tracking," in *Proceedings of the AAAI Conference on Artificial Intelligence*, vol. 36, pp. 1456–1463, 2022.
- [84] J. Zhao, P. Wu, X. Liu, S. Goudarzi, H. Liu, Y. Xu, and W. Wang, "Audio visual multi-speaker tracking with improved gcf and pmbm filter," *Proc. Interspeech 2022*, pp. 3704–3708, 2022.
- [85] F. Sanabria-Macias, M. Marron-Romera, and J. Macias-Guarasa, "Audiovisual tracking of multiple speakers in smart spaces," *Sensors*, vol. 23, no. 15, p. 6969, 2023.
- [86] Y. Liu, Y. Xu, P. Wu, and W. Wang, "Labelled non-zero diffusion particle flow smc-phd filtering for multi-speaker tracking," *IEEE Transactions on Multimedia*, 2023.
- [87] D. Comaniciu, V. Ramesh, and P. Meer, "Kernel-based object tracking," *IEEE Transactions on pattern analysis and machine intelligence*, vol. 25, no. 5, pp. 564–577, 2003.
- [88] X. Qian, A. Brutti, O. Lanz, M. Omologo, and A. Cavallaro, "Audio-visual tracking of concurrent speakers," *IEEE Transactions on Multimedia*, 2021.
- [89] Y. Li, H. Liu, and H. Tang, "Multi-modal perception attention network with self-supervised learning for audio-visual speaker tracking," *arXiv preprint arXiv:2112.07423*, 2021.
- [90] X. Wu, R. He, Z. Sun, and T. Tan, "A light cnn for deep face representation with noisy labels," *IEEE Transactions on Information Forensics and Security*, vol. 13, no. 11, pp. 2884–2896, 2018.
- [91] J. Li, Y. Wang, C. Wang, Y. Tai, J. Qian, J. Yang, C. Wang, J. Li, and F. Huang, "Dsfid: dual shot face detector," in *Proceedings of the IEEE/CVF Conference on Computer Vision and Pattern Recognition*, pp. 5060–5069, 2019.
- [92] W. Liu, D. Anguelov, D. Erhan, C. Szegedy, S. Reed, C.-Y. Fu, and A. C. Berg, "Ssd: Single shot multibox detector," in *European conference on computer vision*, pp. 21–37, Springer, 2016.
- [93] Z. Cao, T. Simon, S.-E. Wei, and Y. Sheikh, "Realtime multi-person 2d pose estimation using part affinity fields," in *Proceedings of the IEEE conference on computer vision and pattern recognition*, pp. 7291–7299, 2017.
- [94] J. Wilson and M. C. Lin, "Avot: Audio-visual object tracking of multiple objects for robotics," in *2020 IEEE International Conference on Robotics and Automation (ICRA)*, pp. 10045–10051, IEEE, 2020.
- [95] Q. Wang, L. Chai, H. Wu, Z. Nian, S. Niu, S. Zheng, Y. Wang, L. Sun, Y. Fang, J. Pan, *et al.*, "The nerc-slip system for sound event localization and detection of dcase2022 challenge," *DCASE2022 Challenge, Tech. Rep.*, 2022.
- [96] J. Bromley, I. Guyon, Y. LeCun, E. Säckinger, and R. Shah, "Signature verification using a siamese time delay neural network," *Advances in neural information processing systems*, vol. 6, 1993.
- [97] L. Bertinetto, J. Valmadre, J. F. Henriques, A. Vedaldi, and P. H. Torr, "Fully-convolutional siamese networks for object tracking," in *European conference on computer vision*, pp. 850–865, Springer, 2016.
- [98] C. Knapp and G. Carter, "The generalized correlation method for estimation of time delay," *IEEE transactions on acoustics, speech, and signal processing*, vol. 24, no. 4, pp. 320–327, 1976.
- [99] H. Do, H. F. Silverman, and Y. Yu, "A real-time SRP-PHAT source location implementation using stochastic region contraction (SRC) on a large-aperture microphone array," in *IEEE International Conference on Acoustics, Speech and Signal Processing*, vol. 1, pp. I-121–I-124, 2007.

- [100] M. Omologo and P. Svaizer, "Use of the crosspower-spectrum phase in acoustic event location," *IEEE Transactions on Speech and Audio Processing*, vol. 5, no. 3, pp. 288–292, 1997.
- [101] A. Brutti, M. Omologo, and P. Svaizer, "Localization of multiple speakers based on a two step acoustic map analysis," in *2008 IEEE International Conference on Acoustics, Speech and Signal Processing*, pp. 4349–4352, IEEE, 2008.
- [102] R. Hartley and A. Zisserman, *Multiple view geometry in computer vision*. Cambridge University Press, 2003.
- [103] H. Sawada, R. Mukai, S. Araki, and S. Malcino, "Multiple source localization using independent component analysis," in *2005 IEEE Antennas and Propagation Society International Symposium*, vol. 4, pp. 81–84, IEEE, 2005.
- [104] I. Trowitzsch, C. Schymura, D. Kolossa, and K. Obermayer, "Joining sound event detection and localization through spatial segregation," *IEEE/ACM Transactions on Audio, Speech, and Language Processing*, vol. 28, pp. 487–502, 2019.
- [105] S. Adavanne, A. Politis, and T. Virtanen, "Direction of arrival estimation for multiple sound sources using convolutional recurrent neural network," in *2018 26th European Signal Processing Conference (EUSIPCO)*, pp. 1462–1466, IEEE, 2018.
- [106] J. M. Vera-Diaz, D. Pizarro, and J. Macias-Guarasa, "Towards end-to-end acoustic localization using deep learning: From audio signals to source position coordinates," *Sensors*, vol. 18, no. 10, p. 3418, 2018.
- [107] D. Berghi, A. Hilton, and P. J. B. Jackson, "Visually supervised speaker detection and localization via microphone array," in *IEEE 23rd International Workshop on Multimedia Signal Processing (MMSP)*, 2021.
- [108] X. Xiao, S. Zhao, X. Zhong, D. L. Jones, E. S. Chng, and H. Li, "A learning-based approach to direction of arrival estimation in noisy and reverberant environments," in *IEEE International Conference on Acoustics, Speech and Signal Processing*, pp. 2814–2818, 2015.
- [109] J. M. Vera-Diaz, D. Pizarro, and J. Macias-Guarasa, "Acoustic source localization with deep generalized cross correlations," *Signal Processing*, vol. 187, p. 108169, 2021.
- [110] S. Adavanne, A. Politis, J. Nikunen, and T. Virtanen, "Sound event localization and detection of overlapping sources using convolutional recurrent neural networks," *IEEE Journal of Selected Topics in Signal Processing*, vol. 13, no. 1, pp. 34–48, 2018.
- [111] S. Adavanne, A. Politis, and T. Virtanen, "Localization, detection and tracking of multiple moving sound sources with a convolutional recurrent neural network," *arXiv preprint arXiv:1904.12769*, 2019.
- [112] S. Adavanne, P. Pertilä, and T. Virtanen, "Sound event detection using spatial features and convolutional recurrent neural network," in *2017 IEEE international conference on acoustics, speech and signal processing (ICASSP)*, pp. 771–775, IEEE, 2017.
- [113] H. C. Maruri, P. López-Meyer, J. Huang, J. A. del Hoyo Ontiveros, and H. Lu, "Gcc-phat cross-correlation audio features for simultaneous sound event localization and detection (seld) on multiple rooms," in *Workshop on Detection and Classification of Acoustic Scenes and Events*, 2019.
- [114] D. Berghi and P. J. B. Jackson, "Audio inputs for active speaker detection and localization via microphone array," in *IEEE Workshop on Applications of Signal Processing to Audio and Acoustics*, 2023.
- [115] C. Schymura, T. Ochiai, M. Delcroix, K. Kinoshita, T. Nakatani, S. Araki, and D. Kolossa, "Exploiting attention-based sequence-to-sequence architectures for sound event localization," in *2020 28th European Signal Processing Conference (EUSIPCO)*, pp. 231–235, IEEE, 2021.
- [116] C. Schymura, B. Bönninghoff, T. Ochiai, M. Delcroix, K. Kinoshita, T. Nakatani, S. Araki, and D. Kolossa, "Pilot: Introducing transformers for probabilistic sound event localization," *arXiv preprint arXiv:2106.03903*, 2021.
- [117] A. Vaswani, N. Shazeer, N. Parmar, J. Uszkoreit, L. Jones, A. N. Gomez, L. Kaiser, and I. Polosukhin, "Attention is all you need," *Advances in neural information processing systems*, vol. 30, 2017.
- [118] T. N. T. Nguyen, K. N. Watcharasupat, N. K. Nguyen, D. L. Jones, and W.-S. Gan, "Salsa: Spatial cue-augmented log-spectrogram features for polyphonic sound event localization and detection," *IEEE/ACM Trans. on Audio, Speech, and Language Processing*, vol. 30, pp. 1749–1762, 2022.
- [119] T. N. Tho Nguyen, D. L. Jones, K. N. Watcharasupat, H. Phan, and W.-S. Gan, "SALSA-lite: A fast and effective feature for polyphonic sound event localization and detection with microphone arrays," pp. 716–720, 2022.
- [120] G. Lathoud, J.-M. Odobez, and D. Gatica-Perez, "Av16. 3: An audio-visual corpus for speaker localization and tracking," in *International Workshop on Machine Learning for Multimodal Interaction*, pp. 182–195, Springer, 2004.
- [121] G. Hinton, O. Vinyals, J. Dean, et al., "Distilling the knowledge in a neural network," *arXiv preprint arXiv:1503.02531*, vol. 2, no. 7, 2015.
- [122] J. Zhao, P. Wu, S. Goudarzi, X. Liu, J. Sun, Y. Xu, and W. Wang, "Visually assisted self-supervised audio speaker localization and tracking," in *2022 30th European Signal Processing Conference (EUSIPCO)*, pp. 787–791, IEEE, 2022.
- [123] G. Irie, M. Ostrek, H. Wang, H. Kameoka, A. Kimura, T. Kawanishi, and K. Kashino, "Seeing through sounds: Predicting visual semantic segmentation results from multichannel audio signals," in *ICASSP 2019-2019 IEEE International Conference on Acoustics, Speech and Signal Processing (ICASSP)*, pp. 3961–3964, IEEE, 2019.
- [124] A. B. Vasudevan, D. Dai, and L. Van Gool, "Semantic object prediction and spatial sound super-resolution with binaural sounds," in *European Conference on Computer Vision*, pp. 638–655, Springer, 2020.
- [125] Y. Aytar, C. Vondrick, and A. Torralba, "Soundnet: Learning sound representations from unlabeled video," *Advances in Neural Information Processing Systems*, vol. 29, pp. 892–900, 2016.
- [126] C. Gan, H. Zhao, P. Chen, D. Cox, and A. Torralba, "Self-supervised moving vehicle tracking with stereo sound," in *Proceedings of the IEEE/CVF International Conference on Computer Vision*, pp. 7053–7062, 2019.
- [127] F. R. Valverde, J. V. Hurtado, and A. Valada, "There is more than meets the eye: Self-supervised multi-object detection and tracking with sound by distilling multimodal knowledge," in *Proceedings of the IEEE/CVF Conference on Computer Vision and Pattern Recognition*, pp. 11612–11621, 2021.
- [128] D. Michelsanti, Z.-H. Tan, S.-X. Zhang, Y. Xu, M. Yu, D. Yu, and J. Jensen, "An overview of deep-learning-based audio-visual speech enhancement and separation," *IEEE/ACM Transactions on Audio, Speech, and Language Processing*, 2021.
- [129] X. Wu, Z. Wu, L. Ju, and S. Wang, "Binaural audio-visual localization," in *Proceedings of the AAAI Conference on Artificial Intelligence*, vol. 35, pp. 2961–2968, 2021.
- [130] S. H. Rezatofighi, A. Milan, Z. Zhang, Q. Shi, A. Dick, and I. Reid, "Joint probabilistic data association revisited," in *Proceedings of the IEEE international conference on computer vision*, pp. 3047–3055, 2015.
- [131] C. Kim, F. Li, A. Ciptadi, and J. M. Rehg, "Multiple hypothesis tracking revisited," in *Proceedings of the IEEE international conference on computer vision*, pp. 4696–4704, 2015.
- [132] I. D. Gebru, S. Ba, G. Evangelidis, and R. Horaud, "Tracking the active speaker based on a joint audio-visual observation model," in *Proceedings of the IEEE International Conference on Computer Vision Workshops*, pp. 15–21, 2015.
- [133] A. Deleforge, R. Horaud, Y. Y. Schechner, and L. Girin, "Co-localization of audio sources in images using binaural features and locally-linear regression," *IEEE/ACM Transactions on Audio, Speech, and Language Processing*, vol. 23, no. 4, pp. 718–731, 2015.
- [134] X. Alameda-Pineda, J. Sanchez-Riera, J. Wienke, V. Franc, J. Čech, K. Kulkarni, A. Deleforge, and R. Horaud, "Ravel: An annotated corpus for training robots with audiovisual abilities," *Journal on Multimodal User Interfaces*, vol. 7, no. 1, pp. 79–91, 2013.
- [135] E. Arnaud, H. Christensen, Y.-C. Lu, J. Barker, V. Khalidov, M. Hansard, B. Holveck, H. Mathieu, R. Narasimha, E. Taillant, et al., "The cava corpus: synchronised stereoscopic and binaural datasets with head movements," in *Proceedings of the 10th international conference on Multimodal interfaces*, pp. 109–116, 2008.
- [136] M. Taj, "Surveillance performance evaluation initiative (spevi)—audiovisual people dataset," *Internet: http://www.eecs.qmul.ac.uk/andrea/spevi.html*, 2007.
- [137] J. Carletta, "Announcing the ami meeting corpus," *The ELRA Newsletter*, vol. 11, no. 1, pp. 3–5, 2006.
- [138] D. Mostefa, N. Moreau, K. Choukri, G. Potamianos, S. M. Chu, A. Tyagi, J. R. Casas, J. Turmo, L. Cristoforetti, F. Tobia, et al., "The chil audiovisual corpus for lecture and meeting analysis inside

- smart rooms,” *Language resources and evaluation*, vol. 41, no. 3, pp. 389–407, 2007.
- [139] M. H. Ooi, T. Solomon, Y. Podin, A. Mohan, W. Akin, M. A. Yusuf, S. del Sel, K. M. Kontol, B. F. Lai, D. Clear, *et al.*, “Evaluation of different clinical sample types in diagnosis of human enterovirus 71-associated hand-foot-and-mouth disease,” *Journal of clinical microbiology*, vol. 45, no. 6, pp. 1858–1866, 2007.
- [140] Q. Liu, W. Wang, T. de Campos, P. J. Jackson, and A. Hilton, “Multiple speaker tracking in spatial audio via phd filtering and depth-audio fusion,” *IEEE Transactions on Multimedia*, vol. 20, no. 7, pp. 1767–1780, 2017.
- [141] D. Berghi, M. Volino, and P. J. B. Jackson, “Tragic Talkers: A Shakespearean sound- and light-field dataset for audio-visual machine learning research,” in *European Conference on Visual Media Production*, 2022.
- [142] W. He, P. Motlicek, and J.-M. Odobez, “Deep neural networks for multiple speaker detection and localization,” in *2018 IEEE International Conference on Robotics and Automation (ICRA)*, pp. 74–79, IEEE, 2018.
- [143] A. Perez, V. Sanguineti, P. Morerio, and V. Murino, “Audio-visual model distillation using acoustic images,” in *Proceedings of the IEEE/CVF Winter Conference on Applications of Computer Vision*, pp. 2854–2863, 2020.
- [144] J. Donley, V. Tourbabin, J.-S. Lee, M. Broyles, H. Jiang, J. Shen, M. Pantic, V. K. Ithapu, and R. Mehra, “Easycom: An augmented reality dataset to support algorithms for easy communication in noisy environments,” *arXiv preprint arXiv:2107.04174*, 2021.
- [145] D. Schuhmacher, B.-T. Vo, and B.-N. Vo, “A consistent metric for performance evaluation of multi-object filters,” *IEEE transactions on signal processing*, vol. 56, no. 8, pp. 3447–3457, 2008.
- [146] K. Bernardin and R. Stiefelhagen, “Evaluating multiple object tracking performance: the clear mot metrics,” *EURASIP Journal on Image and Video Processing*, vol. 2008, pp. 1–10, 2008.
- [147] J. Luiten, A. Osep, P. Dendorfer, P. Torr, A. Geiger, L. Leal-Taixé, and B. Leibe, “Hota: A higher order metric for evaluating multi-object tracking,” *International journal of computer vision*, vol. 129, no. 2, pp. 548–578, 2021.
- [148] Y. Luo and N. Mesgarani, “Tasnet: time-domain audio separation network for real-time, single-channel speech separation,” in *2018 IEEE International Conference on Acoustics, Speech and Signal Processing (ICASSP)*, pp. 696–700, IEEE, 2018.
- [149] Q. Wang, H. Muckenhirn, K. Wilson, P. Sridhar, Z. Wu, J. Hershey, R. A. Saurous, R. J. Weiss, Y. Jia, and I. L. Moreno, “Voicefilter: Targeted voice separation by speaker-conditioned spectrogram masking,” *arXiv preprint arXiv:1810.04826*, 2018.
- [150] J. Ong, B. T. Vo, S. E. Nordholm, B. N. Vo, D. Moratuwage, and C. Shim, “Audio-visual based online multi-source separation,” *IEEE/ACM Transactions on Audio, Speech, and Language Processing*, 2022.
- [151] S. E. Nordholm, H. H. Dam, C. C. Lai, and E. A. Lehmann, “Broadband beamforming and optimization,” in *Academic Press Library in Signal Processing*, vol. 3, pp. 553–598, Elsevier, 2014.
- [152] A. S. Subramanian, C. Weng, S. Watanabe, M. Yu, Y. Xu, S.-X. Zhang, and D. Yu, “Directional asr: A new paradigm for e2e multi-speaker speech recognition with source localization,” in *ICASSP 2021-2021 IEEE International Conference on Acoustics, Speech and Signal Processing (ICASSP)*, pp. 8433–8437, IEEE, 2021.
- [153] Z.-Q. Wang, X. Zhang, and D. Wang, “Robust speaker localization guided by deep learning-based time-frequency masking,” *IEEE/ACM Transactions on Audio, Speech, and Language Processing*, vol. 27, no. 1, pp. 178–188, 2018.
- [154] A. S. Subramanian, C. Weng, S. Watanabe, M. Yu, and D. Yu, “Deep learning based multi-source localization with source splitting and its effectiveness in multi-talker speech recognition,” *Computer Speech & Language*, vol. 75, p. 101360, 2022.
- [155] Y. Chen, X. Qian, Z. Pan, K. Chen, and H. Li, “Locselect: Target speaker localization with an auditory selective hearing mechanism,” *arXiv preprint arXiv:2310.10497*, 2023.
- [156] S. Bhatti and J. Xu, “Survey of target tracking protocols using wireless sensor network,” in *Fifth International Conference on Wireless and Mobile Communications*, pp. 110–115, IEEE, 2009.
- [157] S. Wang and A. Dekorsy, “Distributed consensus-based extended kalman filtering: A bayesian perspective,” in *2019 27th European Signal Processing Conference (EUSIPCO)*, pp. 1–5, 2019.
- [158] H. Rezaei, R. Mahboobi Esfanjani, A. Akbari, and M. H. Sedaaghi, “Event-triggered distributed kalman filter with consensus on estimation for state-saturated systems,” *International Journal of Robust and Nonlinear Control*, vol. 30, no. 18, pp. 8327–8339, 2020.
- [159] K. Ma, L. Xu, and H. Fan, “Unscented kalman filtering for target tracking systems with packet dropout compensation,” *IET Control Theory & Applications*, vol. 13, no. 12, pp. 1901–1908, 2019.
- [160] P. Wu, J. Zhao, S. Goudarzi, and W. Wang, “Partial arithmetic consensus based distributed intensity particle flow smc-phd filter for multi-target tracking,” in *ICASSP 2022-2022 IEEE International Conference on Acoustics, Speech and Signal Processing (ICASSP)*, pp. 5078–5082, IEEE, 2022.
- [161] D. Damen, H. Doughty, G. M. Farinella, S. Fidler, A. Furnari, E. Kazakos, D. Moltisanti, J. Munro, T. Perrett, W. Price, *et al.*, “Scaling egocentric vision: The epic-kitchens dataset,” in *Proceedings of the European Conference on Computer Vision (ECCV)*, pp. 720–736, 2018.
- [162] K. Grauman, A. Westbury, E. Byrne, Z. Chavis, A. Furnari, R. Girdhar, J. Hamburger, H. Jiang, M. Liu, X. Liu, *et al.*, “Ego4d: Around the world in 3,000 hours of egocentric video,” in *Proceedings of the IEEE/CVF Conference on Computer Vision and Pattern Recognition*, pp. 18995–19012, 2022.
- [163] J. Zhao, Y. Xu, X. Qian, and W. Wang, “Audio visual speaker localization from egocentric views,” *arXiv preprint arXiv:2309.16308*, 2023.
- [164] X. Wang *et al.*, “Towards more flexible and accurate object tracking with natural language: Algorithms and benchmark,” in *Proceedings of the IEEE/CVF Conference on Computer Vision and Pattern Recognition*, pp. 13763–13773, 2021.
- [165] Y. Jiang *et al.*, “Prompt-driven target speech diarization,” *arXiv preprint arXiv:2310.14823*, 2023.